AD-A033 496 JOHNS HOPKINS UNIV LAUREL MD APPLIED PHYSICS LAB F/G 20/13
DEVELOPED CONVECTIVE THERMAL FIELDS IN NONCIRCULAR DUCTS.(U)
SEP 76 V O'BRIEN
UNCLASSIFIED APL/JHU/TG-1303 N00017-72-C-4401
NL

1 OF 1
AD
A033496

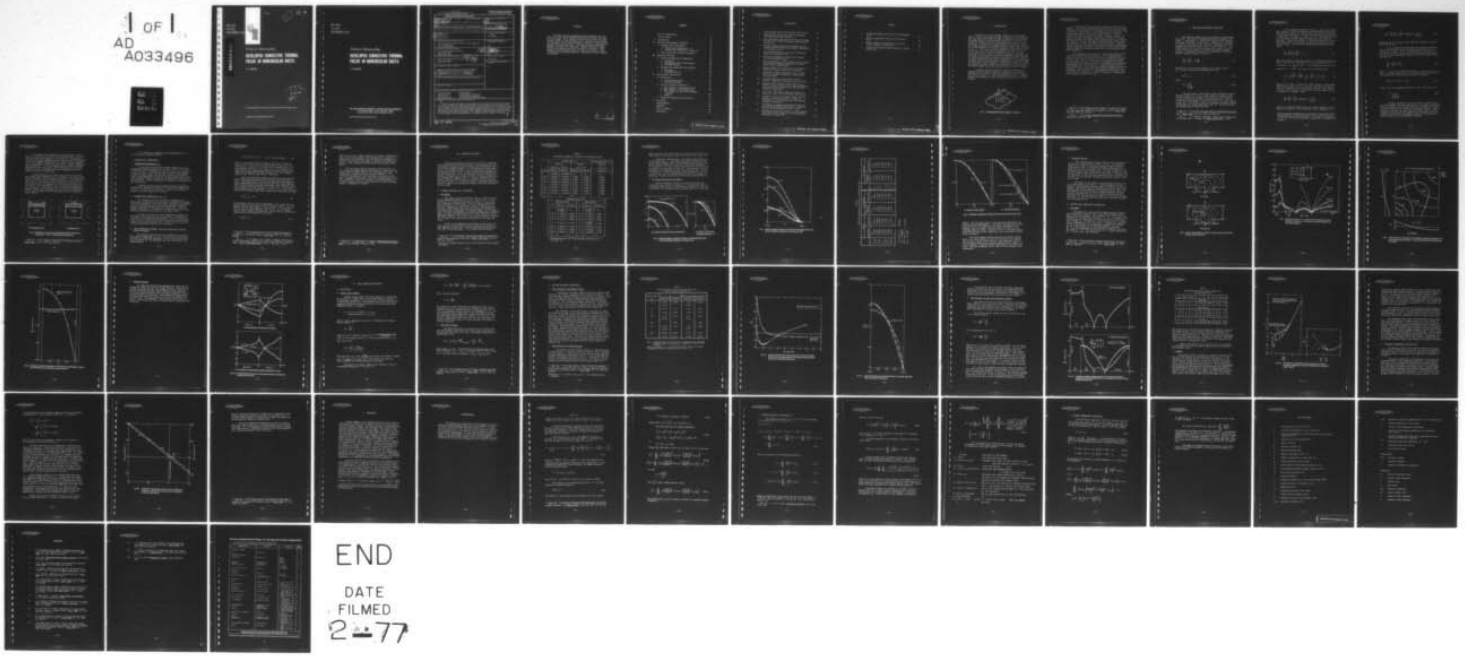

END

DATE
FILMED
2-77

APL/JHU
TG 1303
SEPTEMBER 1976

Technical Memorandum

DEVELOPED CONVECTIVE THERMAL FIELDS IN NONCIRCULAR DUCTS

V. O'BRIEN

THE JOHNS HOPKINS UNIVERSITY ■ APPLIED PHYSICS LABORATORY

APL/JHU
TG 1303
SEPTEMBER 1976

Technical Memorandum

DEVELOPED CONVECTIVE THERMAL FIELDS IN NONCIRCULAR DUCTS

V. O'BRIEN

THE JOHNS HOPKINS UNIVERSITY ■ APPLIED PHYSICS LABORATORY
Johns Hopkins Road, Laurel, Maryland 20810
Operating under Contract N00017-72-C-4401 with the Department of the Navy

Unclassified

SECURITY CLASSIFICATION OF THIS PAGE

PLEASE FOLD BACK IF NOT NEEDED FOR BIBLIOGRAPHIC PURPOSES

REPORT DOCUMENTATION PAGE

1. REPORT NUMBER (14) APL/JHU/TG-1303	2. GOVT ACCESSION NO
3. RECIPIENT'S CATALOG NUMBER (9)	
4. TITLE (*and Subtitle*) (6) DEVELOPED CONVECTIVE THERMAL FIELDS IN NONCIRCULAR DUCTS.	5. TYPE OF REPORT & PERIOD COVERED Technical Memorandum.
	6. PERFORMING ORG. REPORT NUMBER
7. AUTHOR(s) (10) V. O'Brien	8. CONTRACT OR GRANT NUMBER(s) 72 N00017-C-4401
9. PERFORMING ORGANIZATION NAME & ADDRESS The Johns Hopkins University Applied Physics Laboratory Johns Hopkins Road Laurel, Maryland 20810	10. PROGRAM ELEMENT, PROJECT, TASK AREA & WORK UNIT NUMBERS X81K
11. CONTROLLING OFFICE NAME & ADDRESS Naval Plant Representative Office Johns Hopkins Road Laurel, MD 20810	12. REPORT DATE (11) Sep[redacted]76
	13. NUMBER OF PAGES 61
14. MONITORING AGENCY NAME & ADDRESS Naval Plant Representative Office Johns Hopkins Road Laurel, MD 20810 (12) 57p.	15. SECURITY CLASS. (*of this report*) Unclassified
	15a. DECLASSIFICATION/DOWNGRADING SCHEDULE na
16. DISTRIBUTION STATEMENT (*of this Report*) Approved for public release; distribution unlimited (15) N00017-72-C-4401	
17. DISTRIBUTION STATEMENT (*of the abstract entered in Block 20, if different from Report*) na	
18. SUPPLEMENTARY NOTES na	

19. KEY WORDS (*Continue on reverse side if necessary and identify by block number*)

Noncircular ducts	Forced transfer
Convective fields	Incompressible viscous flow
Heat transfer	Finite-difference solutions
Numerical solutions	Fully developed temperature fields

20. ABSTRACT (*Continue on reverse side if necessary and identify by block number*)

Efficient numerical programs of great generality are utilized for steady forced transfer problems with constant heat input per unit length. Fully developed coupled velocity and convective thermal fields for long straight ducts of arbitrary cross-sections are obtained by direct finite-difference solution of the governing momentum and energy equations. Arbitrary Dirichlet temperature boundary conditions are considered. Example solutions of simple sections are compared favorably with analytic solutions. Other examples include extended surfaces more typical of some contemporary heat exchange channels. Application to heat transfer is discussed.

DD FORM 1 JAN 73 1473

Unclassified 031 650 LB

SECURITY CLASSIFICATION OF THIS PAGE

THE JOHNS HOPKINS UNIVERSITY
APPLIED PHYSICS LABORATORY
LAUREL, MARYLAND

ABSTRACT

Efficient numerical programs of great generality are utilized for steady forced transfer problems with constant heat input per unit length. Fully developed coupled velocity and convective thermal fields for long straight ducts of arbitrary cross sections are obtained by direct finite-difference solution of the governing momentum and energy equations. Arbitrary Dirichlet temperature boundary conditions are considered. Example solutions of simple sections are compared favorably with analytic solutions. Other examples include extended surface sections more typical of some contemporary heat exchange channels. Application to heat transfer is discussed.

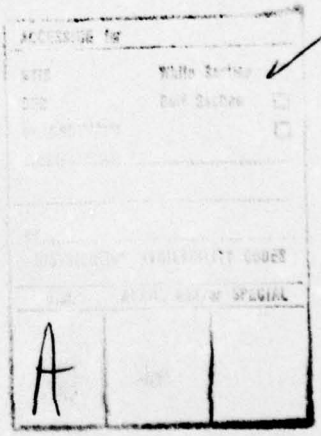

CONTENTS

ILLUSTRATIONS

TABLES

I. INTRODUCTION

Prediction of forced thermal transport in long straight ducts of various cross sections (Fig. 1) has long been sought theoretically since many shapes are used in different cooling arrays. The possibilities of closed analytic solution have not yet been completely exhausted for fully developed thermal fields, but the complexity of thermal field solution tends to increase as the section shape deviates from a simple circle or a planar gap. This is due to the complexity of the fully developed laminar velocity field in the duct. The convective heat transfer is controlled by this velocity field so the resulting thermal field, when it can be found analytically, is also a complicated solution in general. In principle, an exact analytic solution is desirable, but in practical application extensive computer calculations are often required to evaluate quantities that can be compared with usual average measurements, much less point-by-point measurements. Many duct shapes are intractable to exact analysis. This report shows how to employ the computer in direct fashion to obtain accurate solutions for arbitrarily shaped ducts and various Dirichlet boundary conditions.

A thermal convective field solution will depend on the assigned thermal boundary conditions. Constant heat input (or withdrawal) per unit duct length is hypothesized as it is compatible with the concept of a fully developed field (below). Various temperature conditions at the cross-section perimeter will be considered.

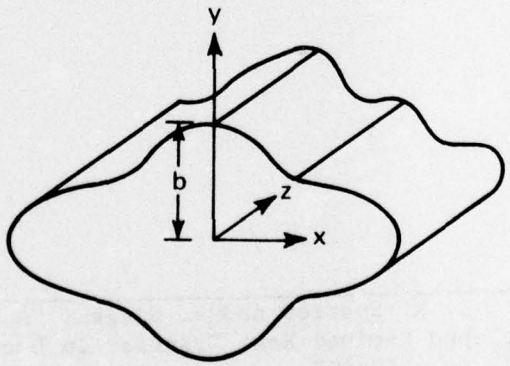

Fig. 1 Long Straight Ducts with Irregular Cross Section

A fully developed steady-state temperature field has been assumed. This implies a great distance from the section where the temperature conditions were first imposed (just as the fully developed velocity field implies a long passage from the entrance). In engineering parlance, the theory applies properly to lengths greater than the hydrodynamic and thermal entrance lengths. The theoretical velocity field is rigorously a condition of minimum pressure drop per unit length, and it appears that the corresponding thermal field also represents a minimum Nusselt number situation (see Ref. 1, especially Discussion by Reynolds). Together the fields provide far downstream asymptotic limits for developing fields. Extensive theoretical calculations of development are beyond the range of the present report but are within today's computer capability.

The equations for the physical fields studied here all involve the well-known Laplace operator. The finite-difference numerical solutions with constant peripheral temperature are compared to exact analytic results (some new) for the same sections to verify their accuracy. The method is extended to more arbitrary sections with extended surfaces resembling some contemporary heat exchange channels for which no analytic solutions have yet been demonstrated. Other temperature boundary conditions also are considered. The calculation of heat transfer quantities used in experimental measurements is straightforward and efficient. The techniques and conclusions are just as relevant to corresponding mass transport problems (Ref. 2).

Ref. 1. E. M. Sparrow and R. Siegel, "A Variational Method for Fully Developed Laminar Heat Transfer in Ducts," Trans. ASME, Vol. 79C, 1959, pp. 157-167.

Ref. 2. W. M. Kays, Convective Heat and Mass Transfer, McGraw Hill, New York, 1966.

II. EQUATIONS AND BOUNDARY CONDITIONS

The physical problems will be idealized to constant property fluid. The fluid is incompressible and has Newtonian viscosity μ and density ρ. Frictional heating will be neglected. The thermal properties, diffusivity α, conductivity k, and specific heat c_p of the fluid are constant. The geometries will be straight and infinitely long in the z direction (Fig. 1). The steady laminar flow is fully developed, i.e., there is only one (z-ward) velocity component u, and the longitudinal pressure gradient is constant and uniform over the section. The single component momentum equation reduces to

$$\frac{\partial^2 u}{\partial x^2} + \frac{\partial^2 u}{\partial y^2} = -\frac{1}{\mu}\frac{dp}{dz} \quad . \tag{1}$$

Normalizing by the duct half-height in the central plane, b, Eq. (1) may be rewritten in nondimensional form

$$\nabla^2 u^* = -1 \tag{1a}$$

where

$$u^* \equiv \frac{u}{\frac{b^2}{\mu}\frac{dp}{dz}} \quad . \tag{1b}$$

Many solutions to this equation (with the nonslip viscous boundary condition $u^* = 0$ on the duct wall) for various cross-sectional shapes are available, some analytical, some numerical. In principle, the velocity field for any shaped duct can be obtained via transformation of the cross section to a circle (Ref. 3). In practice, it is easier to work in a Cartesian coordinate system and provide the solution numerically (Ref. 4). The finite-difference systems are all solved directly.

Ref. 3. L. N. Tao, "On Some Laminar Forced-Convection Problems," Trans. ASME, Vol. 83C, 1961, pp. 446-472.

Ref. 4. V. O'Brien, "Steady and Unsteady Flow in Non-Circular Straight Ducts" (accepted by ASME J. Appl. Mech., 1976).

A fully developed temperature field t with $\partial t/\partial z$ constant with respect to both flow length and cross-sectional position has been specified earlier for constant heat input per unit length and constant wall temperature. We note these are idealizations, and it is permissible to extend the concept of a fully developed field to the cases where the heat input or temperature vary around the perimeter. Using the subscripts w for wall and ref for a reference temperature at the section, along with an overbar for sectional average,† a generalized fully developed thermal field requires

$$\left[\frac{\partial}{\partial z}\left(\frac{\bar{t}_w - t}{t_{ref}}\right)\right] = 0 \quad . \tag{2}$$

Often the reference temperature is $(\bar{t}_w - t_b)$ where the bulk (mixed mean or "mixing-cup") temperature for the cross-sectional area A is defined: $t_b \equiv \frac{1}{\bar{u}A}\int_A ut\, dxdy$. It is assumed that $\bar{t}_w$ and t_b are functions of z only. Carrying out the differentiation,

$$\frac{1}{\bar{t}_w - t_b}\left(\frac{d\bar{t}_w}{dz} - \frac{dt_b}{dz}\right) = \frac{1}{\bar{t}_w - t}\frac{d\bar{t}_w}{dz} - \frac{1}{\bar{t}_w - t}\frac{\partial t}{\partial z} \quad . \tag{3}$$

Since for the case of constant heat input neither of these right-hand terms is equal to zero, $\partial t/\partial z$ must equal $d\bar{t}_w/dz$ in order to cancel the dependence on cross-sectional position. Then $d\bar{t}_w/dz = dt_b/dz$, and by doing an energy balance per unit length of channel dt_b/dz is a constant. Thus

$$\frac{\partial t}{\partial z} = \frac{d\bar{t}_w}{dz} = \frac{dt_b}{dz} = \text{Constant} = \frac{Q}{(A)\rho c_p \bar{u}} \quad , \tag{4}$$

where Q = volume heat addition per unit channel length. If t_w is absolutely constant, on the other hand, and not dependent on z,

†If the quantity is defined for every point of the section, the overbar represents an area average; if the quantity is defined on the wall, the overbar represents a perimeter (circumferential) average.

$$\frac{\partial t}{\partial z} = \frac{t_w - t}{t_w - t_b} \times \frac{dt_b}{dz} = \text{Constant} = \frac{Q}{(A)\rho c_p \bar{u}} \tag{5}$$

Then dt_b/dz is not constant, and a numerical solution is more involved (see below).

It is customary in forced convection problems to neglect the heat diffusion in the flow direction and natural (free) convection due to gravity force. We also assume no internal heat sources in the fluid. The steady thermal transport equation for a fully developed temperature field is a form of the energy equation (Ref. 1).

$$\frac{\partial^2 t}{\partial x^2} + \frac{\partial^2 t}{\partial y^2} = \frac{u}{\alpha} \frac{\partial t}{\partial z} \quad , \tag{6}$$

where $\alpha = k/\rho c_p$ is the thermal diffusivity. Because $\partial t/\partial z$ is constant, a normalized equation for the thermal field appropriate for the constant heat input per unit length can be written

$$\nabla^2 t^* = u^* = \nabla^2 (t^* - \bar{t}_w^*) \quad , \tag{6a}$$

where t^* has been nondimensionalized, via Eqs. (1b) and (4), as

$$t^* = \frac{t}{\frac{b^4}{\mu\alpha} \frac{dp}{dz} \frac{\partial t}{\partial z}} \tag{6b}$$

Successful development of practical heat transfer theory requires boundary conditions appropriate to the physical situations. Most prior efforts have involved homogeneous boundary conditions, which has simplified the mathematical algebraic analysis. However, taking into account that there can occur problems where uniform boundary values are not valid assumptions, the present numerical programs allow arbitrary peripheral temperature distributions to match a variety of cooling (heating) problems.

For example, many applications of cooling ducts involve an array of identical ducts through a hot material matrix. Unless they are lined with a material of very high heat conductivity, it is unlikely that the embedded ducts will have uniform wall temperature. The peripheral temperature will depend on the arrangement of the ducts within the material to be cooled. Figure 2 shows two such arrangements. If the homogeneous matrix contains uniformly distributed heat sources (e.g., from radioactivity or exothermic chemical reaction), probable temperature distributions on the walls of the ducts are indicated.

Uniform flux per unit surface area at the wall has also been a theoretical assumption that is unlikely to be found in noncircular open duct forced transfer application. For extended surfaces, the probabilities of uniform temperature or flux are even less (Ref. 5). The present program allows any assigned temperature distribution to be applied as the duct wall boundary condition (B.C.). The considerable effects of nonuniform temperature are illustrated. (In principle, one can solve the nonhomogeneous boundary value problem algebraically as well [see the appendix], but the effects seem not to have been shown even for relatively simple shapes.)

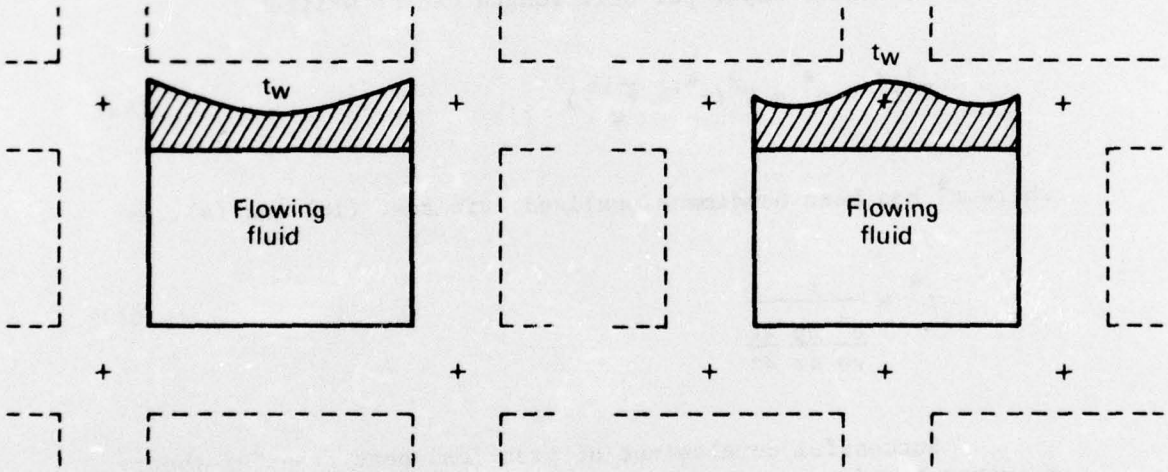

Fig. 2 Different Duct Arrays with Indicated Possible Wall Temperature Distributions. Cross (+) marks local peak temperature.

Ref. 5. K. A. Gardner, "Efficiency of Extended Surface," Trans. ASME, Vol. 67, 1945, pp. 621-627.

For convenience, homogeneous and nonhomogeneous B.C.'s are discussed in separate sections.

A. ASSIGNED WALL TEMPERATURES

1. Uniform Wall Temperature, t_w

For sectionally uniform but linearly varying $t_w(z)$, the homogeneous boundary condition for Eq. (6a) is $\theta^* \equiv t^* - t_w^* = 0$ on the duct wall. An analytic solution for a square duct based on a recent solution of the velocity field is given in the appendix. It will be used to assess the absolute accuracy of the present direct finite-difference solution of the same problem (and to provide an analytic basis for comparison of the effect of other boundary conditions). Other rectangular duct shapes are considered, as are curved walls.

Advantage has been taken of assumed bilateral symmetry to consider just one-quarter of the field. This saves computer time but is not a fundamental requirement. Similar calculations are possible with more irregular duct shapes.

2. Variable Wall Temperature $t_w(X_w, Y_w)$

If the material of the duct walls is homogeneous and source-free, and has high heat conductivity, uniform t_w^* is probably a valid assumption. For other cases, temperature distributions on the duct section perimeter provide more general "arbitrary" boundary conditions on the convective thermal field. The only physical constraint on the generality is that the profile be continuous, particularly at corners of rectangular ducts.

An analytic solution for simple temperature profiles on the edges of the square duct has been derived for comparison to the numerical solution (see the appendix). Due to the linearity of Eq. (6), the solution consists of the sum of the solution discussed in the previous section and a solution satisfying the nonconstant temperature condition on the perimeter.

B. OTHER THEORETICAL BOUNDARY CONDITIONS (PREVIOUSLY USED FOR CERTAIN PROBLEMS)

The condition that the duct wall temperature be an absolute constant independent of x, y, or z has also been used theoretically for simple duct problems. This is a very special case. For t_w constant, Eq. (5) substituted into Eq. (6) reduces it to (approximately)

$$(\nabla^2 + b'u^*)t = a'u^* \qquad (a',b' \text{ are constants}). \qquad (7)$$

This is a more complex equation than Eq. (6a) and, although the operator $(\nabla^2 + b'u^*)$ can be iterated numerically (Ref. 6), such solutions for noncircular ducts will not be considered here. The wall boundary condition is, of course, $t = t_w$. Previously published results for simple shapes show this boundary condition provides less efficient average heat transfer (i.e., lower Nusselt numbers) than variable $t_w(z)$ (Ref. 2, Table 8-2).

Some fully developed temperature fields have been analyzed with assigned piecewise uniform flux boundary conditions (Refs. 1 and 7). Rectangular duct solutions were obtained by separating the total temperature solution into two portions. The first takes an analytic form exactly satisfying the assigned flux condition (gradient or Neumann condition) and Eq. (6) — call it t_f. This reduced the second portion of the solution — call it t_0 — to a zero flux condition on the boundary which had to satisfy (in the present notation)

$$\nabla^2 t_0^* = u^* - \bar{u}^*. \qquad (8)$$

The rectangular solution t_0^* is independent of the actual flux conditions (such as given relative flux on alternate sides). For less regular sections (nonrectangular, noncircular), it is more difficult to find the exact (analytic) flux portion, t_f, for uniform flux (or other assigned distributions). This portion is constrained (mathematically and physically) to satisfy

$$\nabla^2 t_f^* = \bar{u}^* \qquad (9)$$

Ref. 6. S. H. Clark and W. M. Kays, "Laminar-Flow Forced Convection in Rectangular Tubes," Trans. ASME, Vol. 75, 1953, pp. 859-866.

Ref. 7. J. M. Savino and R. Siegel, "Laminar Forced Convection in Rectangular Channels with Unequal Heat Addition on Adjacent Sides," Int. J. Heat Mass Transf., Vol. 7, 1964, pp. 733-741.

Table 14.02 in Ref. 8 may be useful for separable coordinate systems, but the flux boundary value problem is more complicated analytically and numerically than for Dirichlet temperature conditions. With uniform flux boundary conditions on noncircular ducts, the wall temperature varies around the perimeter (Refs. 1 and 7).

The so-called radiation boundary condition $\partial t/\partial n = \lambda t$ (n = normal to surface) has also been used as a theoretical convective field boundary condition for one-dimensional flows. Extending this to noncircular ducts implies $\partial/\partial n(\ell n\ t) = \lambda$ or $t = t_w\ e^{\lambda n}$ uniformly over the fluid region enclosing the duct wall. Generally $\partial u^*/\partial n$ varies around the perimeter while at the wall $\partial/\partial n(\nabla^2 t^*) = \partial^3 t^*/\partial n^3$ = constant by the hypothesized B.C. So this condition does not seem appropriate for fully developed fields in irregular duct shapes.

Ref. 8. P. Moon and D. C. Spencer, Field Theory for Engineers, D. Van Nostrand, Princeton, 1961.

III. NUMERICAL SOLUTIONS

This section presents a survey of the kinds of steady developed convective field solutions that can be obtained directly with computer programs using the Cartesian finite-difference formulation of the Laplace operator, ∇^2. The numerical schemes themselves are variations of Ref. 9 and were discussed very briefly in the appendix of Ref. 4 by Dr. Louis W. Ehrlich who programmed the various problem sets. The fully developed velocity field is obviously an integral part of each solution, but these problems have been considered at length in Ref. 4. Without repeating the discussion, the main point is that the numerical velocity solutions are quite accurate.† As pointed out above, the thermal field solutions will depend upon the thermal boundary conditions assigned on the duct walls.

A. UNIFORM PERIPHERAL WALL TEMPERATURE

1. Rectangles

The complete numerical solution with $h = 1/32$ for the normalized temperature difference $\theta^* = t^* - t_w^*$ with $\theta^* = 0$ on the duct walls for a square is illustrated in Table 1 by the centerplane temperature distributions. Both the absolute temperature and that relative to the calculated central temperature θ_c^* are given for comparison to the analytic solution. The agreement is very good, and if higher digit accuracy is desired a finer mesh solution is easily attainable at a slightly higher cost in computer time. The cost of obtaining the velocity and temperature values at nearly a thousand interior points, $h^{-2} = (32)^2$, was \$2.13 on the IBM 360/91 computer. The cost of evaluating the analytic solutions for 16 points on the central plane was greater on the same computer.

Values of the temperature distribution in the narrow central plane of other rectangular ducts are also given in Table 1. Some comparison values from a previous pioneering numerical solution (Ref. 6) are also shown. It is evident that the profile

---

Ref. 9. L. W. Ehrlich, "Solving the Biharmonic Equation as Coupled Finite Difference Equations," SIAM J. Num. Anal., Vol. 8, 1971, pp. 278-287.

†Illustrative examples showed errors in the fourth or fifth significant digit.

Table 1

Centerplane Temperature Profiles in Rectangular Ducts

	Square (a/b = 1)				Planar gap (a/b = ∞)
	Absolute $\theta^*(0,Y)$ or $\theta^*(X,0)$		Relative $(\theta_c^*)^{-1}\,\theta^*$		Relative $(\theta_c^*)^{-1}\,\theta^*$
Y,(X)	Numerical	Analytic	Numerical	Analytic	Analytic
0	-0.064990	-0.064998	1.0	1.0	1.0
0.125	-0.063841	-0.063848	0.9823	0.9823	0.9813
0.25	-0.060413	-0.060418	0.9296	0.9296	0.9258
0.375	-0.054766	-0.054769	0.8427	0.8426	0.8352
0.5	-0.047010	-0.047011	0.7233	0.7233	0.7125
0.625	-0.037324	-0.037322	0.5743	0.5742	0.5618
0.75	-0.025976	-0.025972	0 3997	0.3996	0.3883
0.875	-0.013353	-0.013348	0.2055	0.2054	0.1985
1.0	0	0	0	0	0

Rectangle (a/b = 2)					
Narrow Profile			Wide Profile		
Y	Absolute	Relative	X	Absolute	Relative
0	-0.162114 -0.1626†	1.0	0	-0.162114 -0.1626†	1.0
0.125	-0.159106	0.9815	0.25	-0.159926	0.9865
0.25	-0.150172	0.9263	0.5	-0.153244	0.9453
0.375	-0.135575	0.8363	0.75	-0.141733	0.8743
0.5	-0.115761	0.7141	1.0	-0.124893 -0.1256†	0.7704
0.625	-0.091364	0.5636	1.25	-0.102199	0.6304
0.75	-0.063212	0.3899	1.5	-0.073340	0.4524
0.875	-0.032340	0.1995	1.75	-0.038678	0.2386
1.0	0	0	2	0	0

†Renormalized value from Clark and Kays relaxation solution (Ref. 6).

shapes are very nearly identical in the narrow central plane; the major variation with aspect ratio a/b is the central value, θ_c^*.

Temperature distributions on the wider central plane are illustrated by Fig. 3. The shape of the profile becomes flatter as the width-to-height ratio = a/b approaches infinity (Fig. 3a). If the relative results are plotted in "stretched coordinates," θ^*/θ_c^* versus $X' = (b/a)X$, it is more evident that the curves are not similar but vary with a/b (Fig. 3b). The variation along the diagonals of the rectangles is also illustrated in Fig. 4, where $S' = 2^{-\frac{1}{2}}[Y^2 + (X')^2]^{\frac{1}{2}}$ is another stretched coordinate. Also included in Fig. 4 is the corresponding profile from a square duct approximate thermal solution via a variational approach (Ref. 1).

2. Ellipses and Other Curved Shapes

Similar numerical results are given for circular and ellipsoidal ducts in Table 2 and Fig. 5. The finite-difference calculations were carried out in Cartesian coordinates. The comparison with the conformal analytic results (Ref. 3) is quite rea-

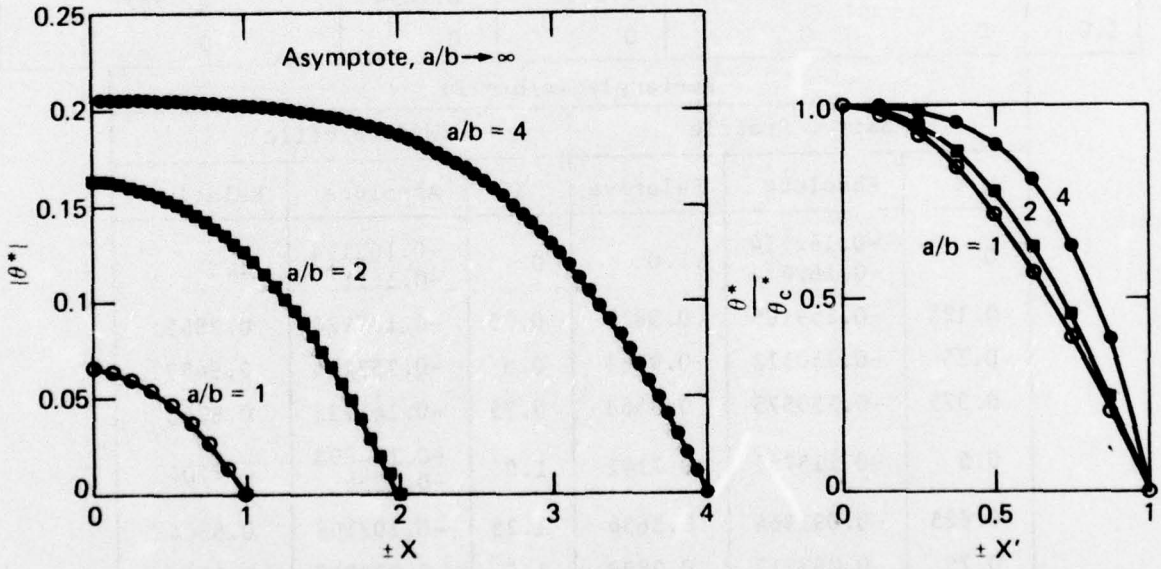

(a) Absolute profile versus horizontal distance

(b) Relative profile versus "stretched coordinate," X'

Fig. 3 Wide Centerplane Temperature Profiles in Rectangular Ducts with Uniform Peripheral Temperature for Several a/b

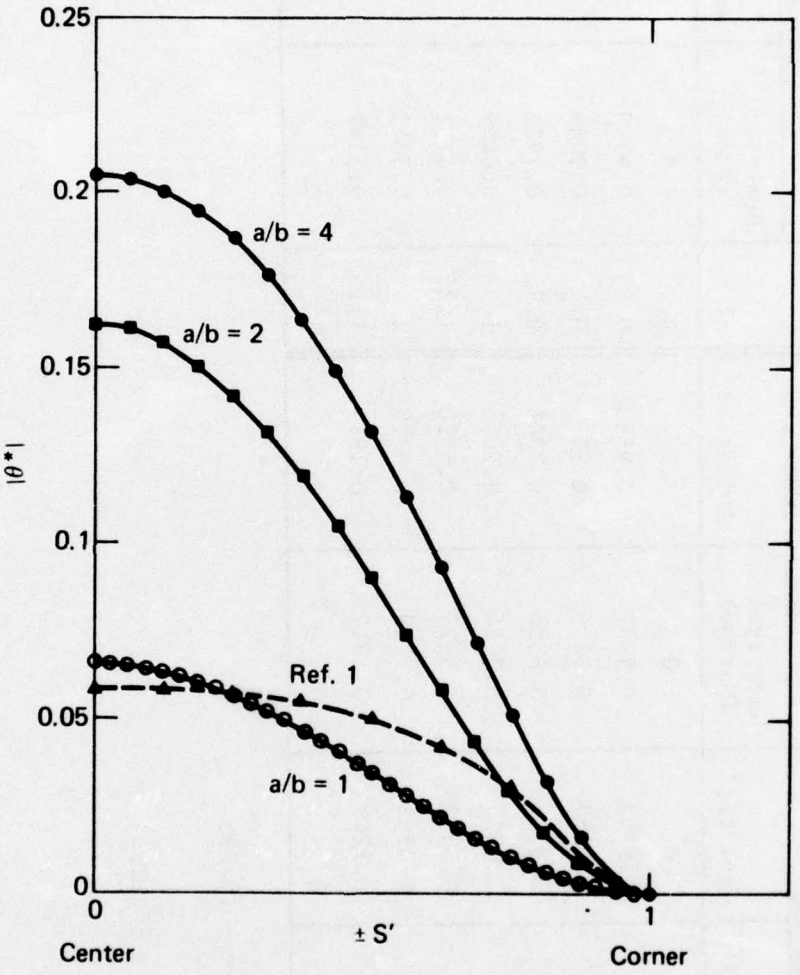

Fig. 4 Absolute Diagonal Temperature Profiles for Rectangular Ducts with Uniform Peripheral Temperature as a Function of a/b

Table 2

Relative Temperature Profiles in Elliptical Ducts

	Circle		2:1 Ellipse			2:1 Ellipse	
Y	Numerical†	Analytic‡	Numerical†† (Narrow)	Analytic‡‡	X	Numerical†† (Wide)	Analytic‡‡
0	1.0	1.0	1.0	1.0	0	1.0	1.0
0.125	0.9793	0.9793	0.9807	0.9813	0.25	0.9758	0.9764
0.25	0.9179	0.9180	0.9235	0.9235	0.5	0.9049	0.9048
0.375	0.8190	0.8191	0.8306	0.8308	0.75	0.7923	0.7924
0.5	0.6876	0.6875	0.7054	0.7055	1	0.6459	0.6460
0.625	0.5301	0.5300	0.5527	0.5528	1.25	0.4772	0.4772
0.75	0.3556	0.3555	0.3789	0.3790	1.5	0.3013	0.3008
0.875	0.1746	0.1746	0.1917	0.1917	1.75	0.1347	0.1347
1.0	0	0	0	0	2	0	0

†$h = (16)^{-1}$, $u_c = -0.04693$

‡$u_c = -0.04688$

††$h = (16)^{-1}$, $u_c = -0.12303$

‡‡$u_c = -0.12293$

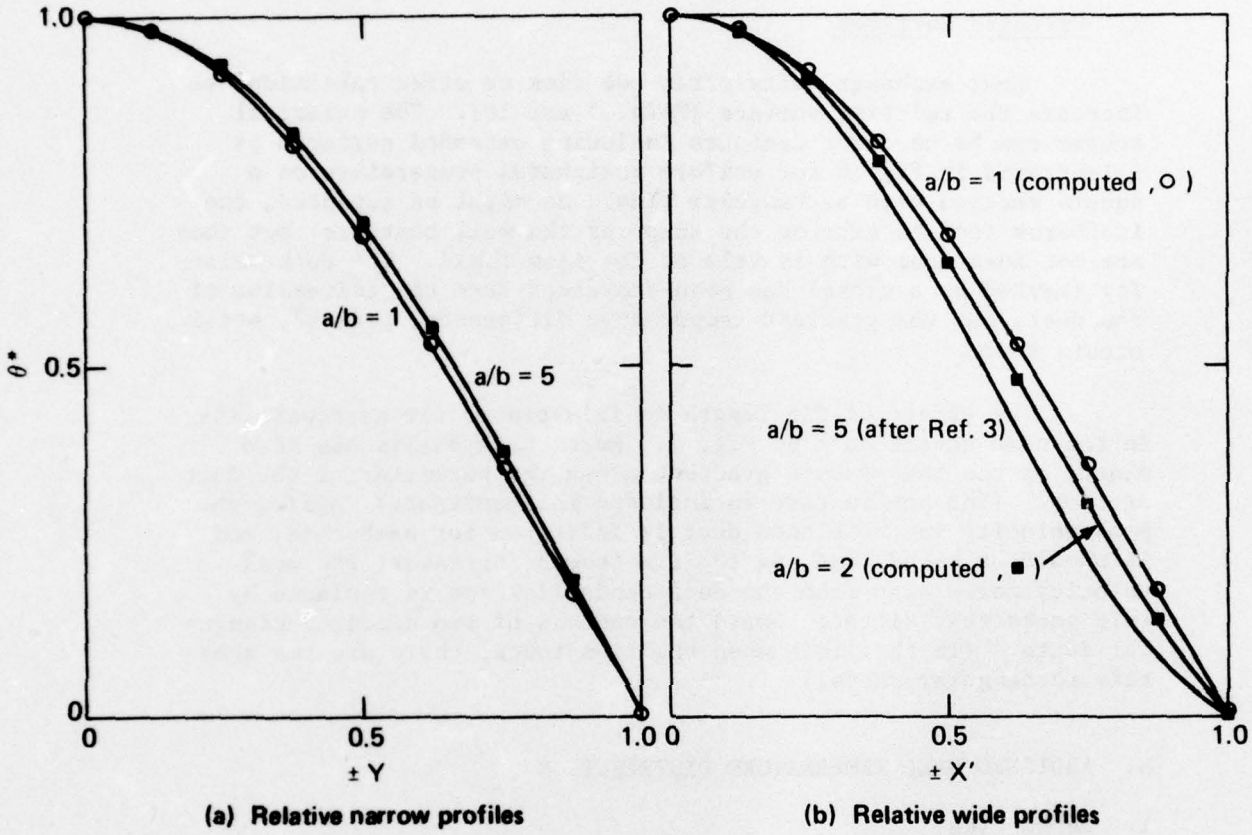

(a) Relative narrow profiles

(b) Relative wide profiles

Fig. 5 Centerplane Temperature Profiles in Elliptical Ducts as a Function of a/b

sonable. (On the scale of Fig. 5, the numerical and analytic results cannot be distinguished.) The narrow central-plane relative profiles, θ^*/θ_c^*, are essentially the same, independent of the semimajor axis ratio (a/b), and very similar to those for the rectangles shown on Table 1. However, as $a/b \to \infty$ the wide centerplane profiles tend to bell-shapes more like the diagonal profiles in the rectangles.

The "short-legged" formulas applied to Cartesian coordinates to get these results for the conic sections can be applied just as well to other curved contours. Any combination of flat and circularly filleted arcs could be handled just as readily. It is not necessary to have an analytic description of the wall contours. The wall coordinates can be read in from rectangular grid measurements.

3. Extended Surfaces

Heat exchange ducts often use fins or other extensions to increase the relative surface (Refs. 5 and 10). The numerical scheme can be used for contours including extended surfaces as illustrated in Fig. 6 for uniform peripheral temperature on a square section with rectangular fins. As might be expected, the isotherms tend to take on the shape of the wall contours, but they are not identical with isovels of the flow field. The peak velocity (marked by a cross) has been displaced from the centerline of the duct, but the greatest temperature difference, peak θ^*, still occurs there.

The effect of fin length is illustrated for narrower fins in the same square duct by Fig. 7. Here the emphasis has been placed on the temperature gradient along the perimeter of the duct section. (The no-fin case is included for contrast.) Again, the peak velocity in the finned duct is indicated for each case, and it should be noted that, as the fin length increases, the peak velocity moves away from the duct centerline and is replaced by twin peaks that migrate toward the centers of two almost rectangular ducts. (In the limit when the fins touch, there are two separate rectangular ducts.)

B. ASSIGNED WALL TEMPERATURE DISTRIBUTION

1. Rectangles

The square duct solution with assigned parabolic temperature distributions along the walls (Fig. 8) was obtained by the direct numerical technique. The average $\theta_w^* = 0$. The results are dependent on a nondimensional parameter ε (see the appendix) that characterizes the magnitude of the nonuniformity but can be positive or negative. The difference from the uniform $\theta_w^* = 0$ problem can be considerable if $|\varepsilon|$ is not small. Isotherms are compared in Fig. 8 and (normal) wall temperature gradients (or flux) in Fig. 9. (The accuracy of the finite-difference calculation ($h = 1/16$) with assigned wall distribution is verified by the center value $\theta_c^* = t_c^* - t_w^*$; analytically $\theta_c^* = -0.5288$, numerically $\theta_c^* = -0.5315$, about 0.5% deviation.)

Ref. 10. M. H. Hu and Y. P. Chang, "Optimization of Finned Tubes for Heat Transfer in Laminar Flow," Trans. ASME, Vol. 95C, 1973, pp. 332-338.

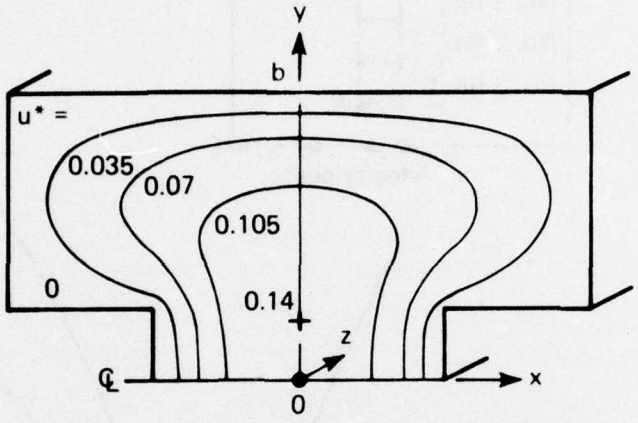

(a) Isovels

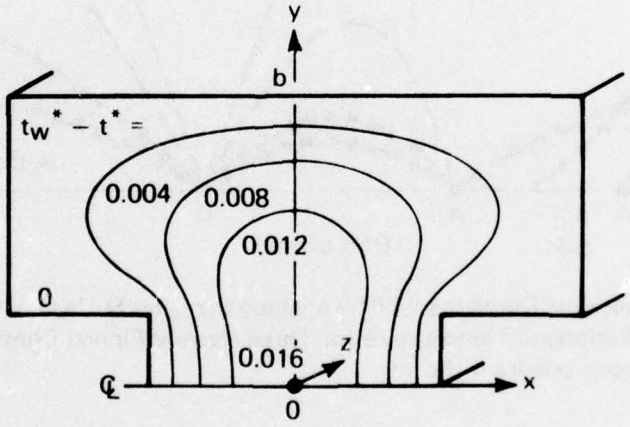

(b) Isotherms

Fig. 6 Velocity and Temperature Fields for a Square Duct with Extended Surfaces (upper half shown)

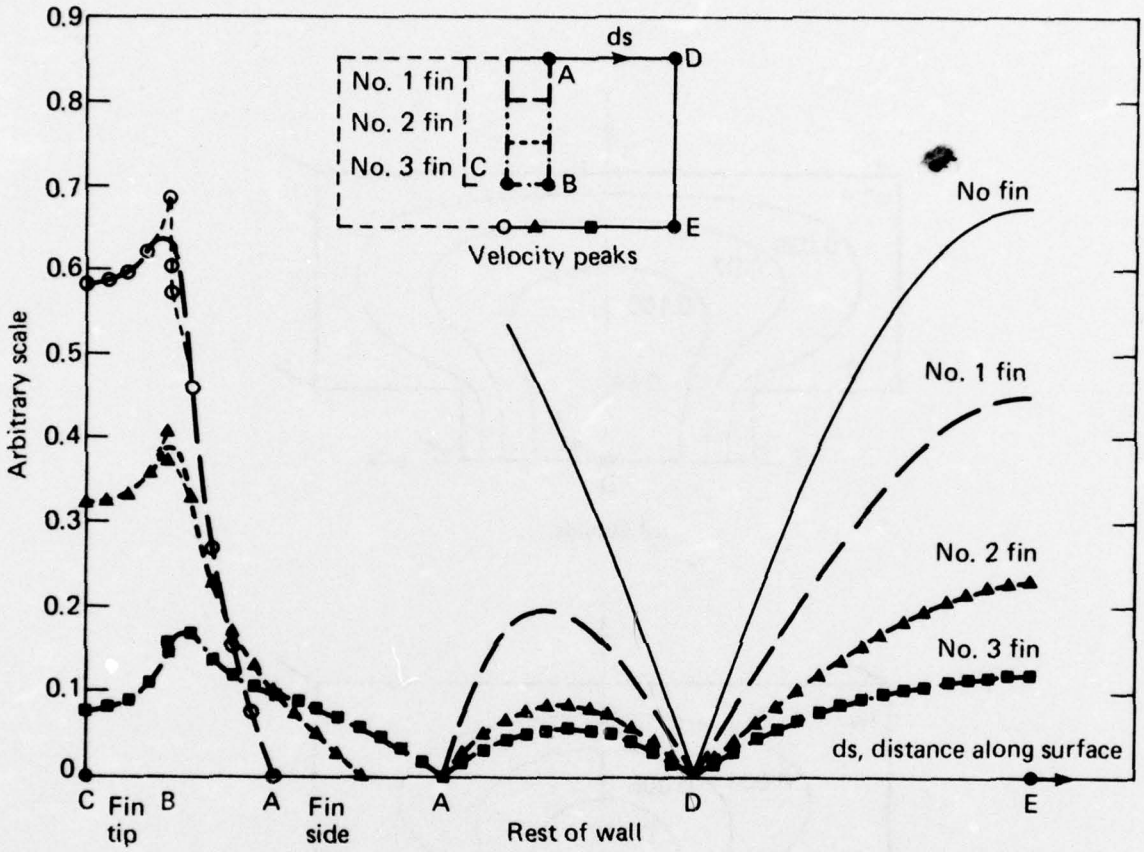

Fig. 7 Normal Derivatives, $\partial\theta^*/\partial n$, along the Duct Surface with Uniform Peripheral Temperature for Three Narrow Finned Configurations (one quadrant shown)

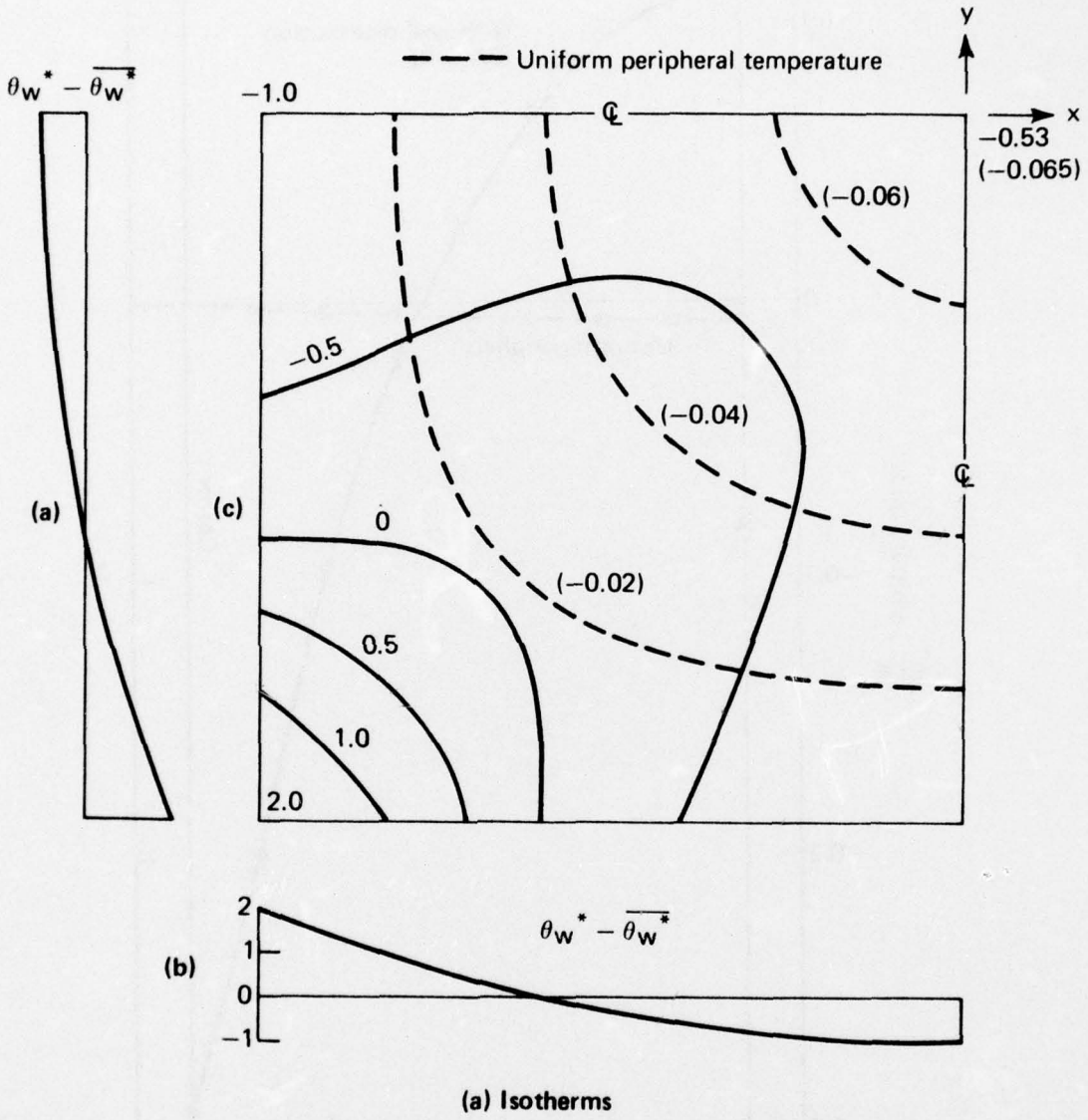

(a) Isotherms

Fig. 8 Thermal Field for a Square Duct with Parabolic Temperature Distributions on the Perimeter (peaks at corners). (a) and (b) Wall temperature distributions; (c) isotherms.

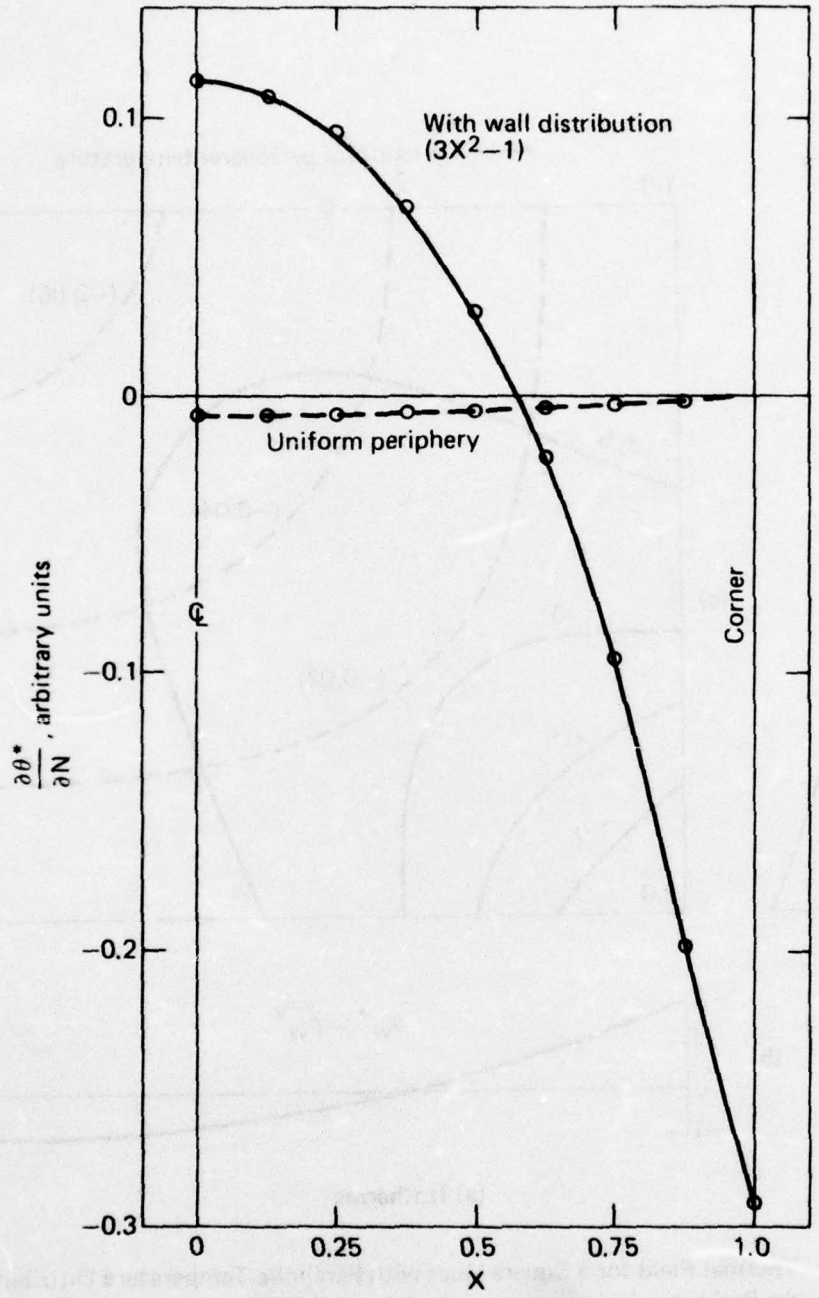

Fig. 9 Temperature Gradient Distribution for a Square Duct with Parabolic Temperature Distributions on the Perimeter (peaks at corners)

2. Extended Surfaces

The numerical solutions with assigned wall values can be extended to curved contours and extended surfaces. Fins with temperature distributions (Fig. 10a) combined with duct walls with a uniform value give distorted thermal fields and very different flux values along the surface (Fig. 10b) when compared to totally uniform peripheral temperatures. The difference in magnitude of the normal derivative is so large the uniform case appears as essentially zero. The parameter β, which is the value at the tip corner, characterizes the effect for these similar temperature distributions.

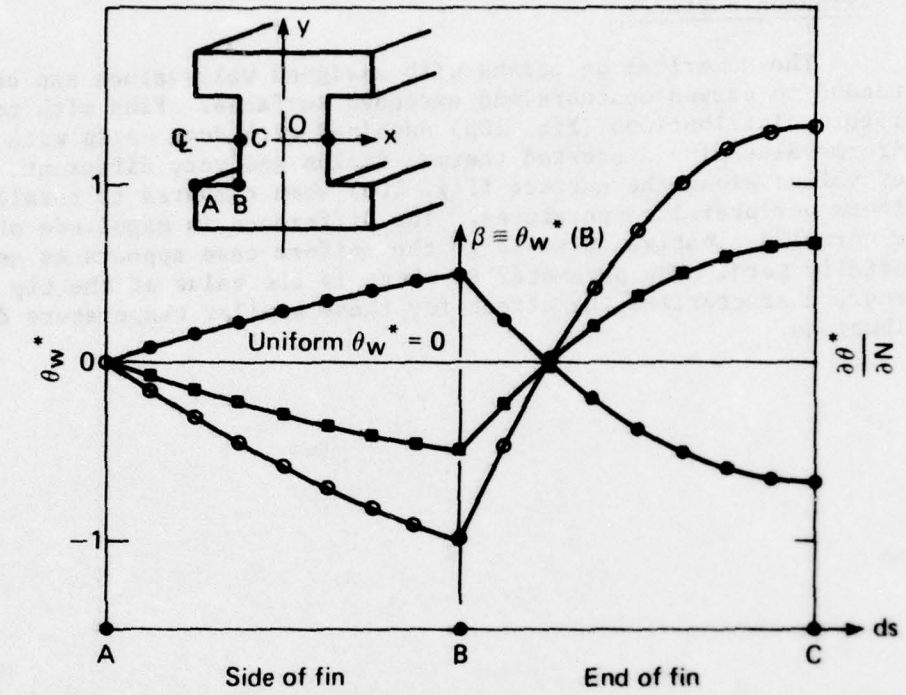

(a) Wall temperature distributions on the fins

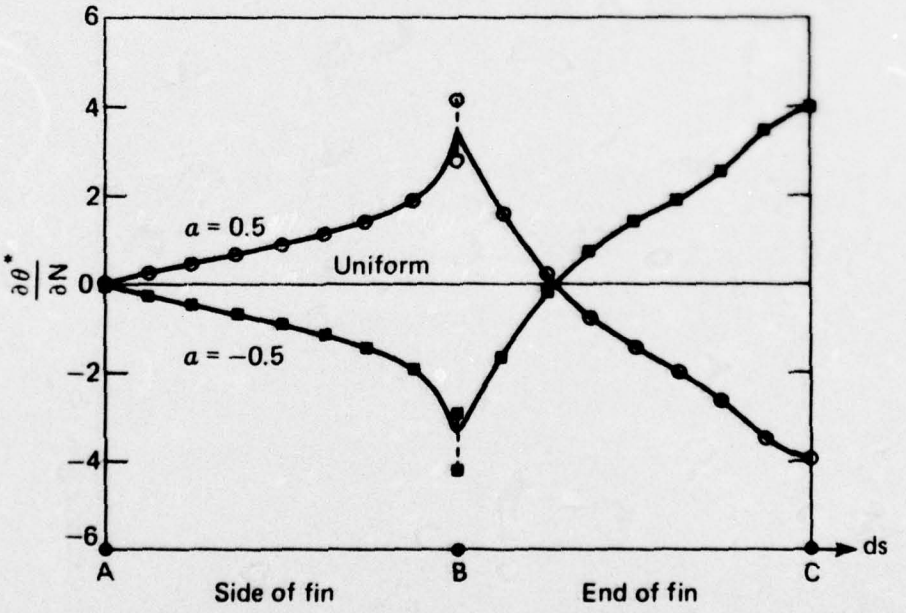

(b) Variation of wall temperature gradient along the fin surface

Fig. 10 A Finned Square Duct with Various Similar Symmetric Temperature Distributions on the Fins

IV. HEAT TRANSFER APPLICATIONS

A. DEFINITIONS

1. Average Heat Transfer

Average thermal fields are usually defined for engineering use in terms of a "mixed mean" or bulk temperature t_b, instead of a simple mean temperature. An average heat transfer conductance h is often based on the total heat transfer rate to the fluid and the temperature difference between the wall of the duct and the bulk temperature (Refs. 1 through 3).

$$h \equiv \frac{Q}{(\text{heated perimeter}) \cdot (t_b - \bar{t}_w)}$$

This is usually expressed in terms of a nondimensional (average) Nusselt number, Nu:

$$Nu \equiv \frac{h\, D_e}{k} \quad ,$$

where D_e is the "hydraulic diameter;" $D_e \equiv \frac{4 \text{ cross-sectional area}}{\text{perimeter}} = \frac{4A}{P}$. In the present notation, for open rectangular ducts of aspect ratio (a/b),

$$Nu = \frac{4\,\bar{u}^*}{\theta_b^*} \frac{(a/b)^2}{(1 + a/b)^2} \quad ,$$

which includes a D_e of $4b \frac{(a/b)}{(1 + a/b)}$ that equals the "geometric diameter," 2b, only for a square duct. This assumes also that the *heated perimeter and wetted perimeter are the same.*

Alternately the Nusselt number can be defined in terms of the geometric diameter, $d = 2b$ $(a/b \geq 1)$,

$$Nu' \equiv \frac{hd}{k} = \frac{(2b)h}{k} = \frac{2\bar{u}^*}{\theta_b^*} \frac{(a/b)}{(1 + a/b)} \quad \text{for rectangles} \quad ,$$

where average conductance

$$h \equiv k \cdot \frac{Nu'}{2b} \quad .$$

The length $k/h = 2(Nu')^{-1}(b)$ has been interpreted (Ref. 11) as a thermal barrier that "represents the thickness of a stationary fluid film having a thermal resistance corresponding to h." For fully developed flow characterized by one coordinate (1-D flow) and uniform peripheral temperature, namely the classic circular duct and planar gap problems, the values of h/k are 2.18 b^{-1} and 2.06 b^{-1}, respectively (see Table 2 in Ref. 11). Thus the 1-D thermal barrier layer seems to be about one-half the distance to the duct centerline.

2. Local Heat Transfer

For some applications, the interest is on the local surface heat-transfer conductance that varies around the perimeter of the noncircular ducts (2-D flow). The surface conductance is defined (Ref. 6) as

$$h_{loc} \equiv \frac{k}{t_b - \bar{t}_w} \left(\frac{\partial t}{\partial n}\right)_{surface} = \frac{k}{b\theta_b^*} \left(\frac{\partial \theta^*}{\partial N}\right)_w \quad ,$$

where normal N is X, Y respectively for alternate sides of an open rectangular duct. If h_{loc} is averaged over the total perimeter P, the mean surface conductance is $\bar{h}_{loc} = \frac{1}{P} \int_P h_{loc}(s)ds$.

Ref. 11. R. N. Norris and D. D. Streid, "Laminar-flow Heat Transfer Coefficients for Ducts," Trans. ASME, Vol. 62, 1940, pp. 525-541.

B. UNIFORM PERIPHERAL TEMPERATURE

1. Heat Transfer in Rectangular Ducts

A compilation of Nusselt number evaluations, numerical and analytic, for various rectangular ducts is given in Table 3. Previous numerical results (see Ref. 2) are enclosed in brackets. The analytic values have been reevaluated with series truncated at a very large number of terms so there are some slight differences from Ref. 12. The conventional Nusselt number, Nu, is monotonic (increasing) with a/b increasing. However, Nu' has a minimum near a/b = 2.† Even so the average thermal barrier layer varies only ±10% from a mean value about $(1.7)^{-1}b$ for $a/b \leq 8$ (Fig. 11).

The variation of normalized surface conductance $h_{loc}/\bar{h}_{loc}$ is illustrated in Fig. 12 for the square duct (compare Fig. 2 in Ref. 12). It has been stated that a numerical solution is not sufficiently accurate to describe the variation adequately (Ref. 6). This statement is usually not accompanied by a direct comparison of a fine mesh calculation and the corresponding analytical evaluation, as here. The figure establishes the engineering utility of direct numerical solutions for local conductance (less than 2% deviation). The variational solution (Ref. 1) is less accurate. For further comparison and physical insight, the shear profile of the velocity field is also shown (dashed curve). The variation of shear and surface conductance with distance along the duct perimeter is rather similar. The peak values are at the center, the average values about 60% of the way to the corner, and both curves fall to zero at the corner. Thus the local thermal barrier layer (inversely proportional to h_{loc}) increases without limit as the sharp concave corner is approached and the velocity shear approaches zero.

2. Heat Transfer in Elliptical Ducts

A discussion of heat-transfer results for elliptical ducts is found in Ref. 3. There is no need to repeat it here. Rectangular and elliptical sections have the same limiting planar gap centerplane temperature distribution as $a/b \to \infty$, but the Nu variation with a/b is different (see Fig. 4, Ref. 5). One-half Nu' and its inverse, the average thermal barrier layer, for elliptical ducts rapidly approach limiting values as a/b increases (Fig. 11).

Ref. 12. S. M. Marco and L. S. Han, "A Note on Limiting Laminar Nusselt Number in Ducts with Constant Temperature Gradient by Analogy to Thin-Plate Theory," Trans. ASME, Vol. 77, 1955, pp. 625-630.

†Minimum Nu'/2 = 1.54613 occurs at a/b = 1.97; maximum barrier = 0.64686 b.

Table 3

Nusselt Numbers for Rectangular Ducts with Uniform Peripheral Temperature

Aspect ratio	Nu		$Nu'/2 \sim (\text{barrier layer})^{-1}$	
a/b	Numerical	Analytic†	Numerical	Analytic
1.0	3.600	3.6079	1.800	1.804
	[3.63]		(1.82)	
1.4	[3.78]	3.734	(1.62)	1.600
1.5	3.787	3.790	1.578	1.579
2.0	4.131	4.123	1.55	1.546
	[4.11]		(1.54)	
3.0		4.795		1.598
4.0	5.365	5.331	1.68	1.666
	[5.35]		(1.67)	
8.0	[6.60]	6.498	(1.85)	1.828
∞	8.235	8.235	2.059	2.059

Note: Bracketed values are from Kays, Convective Heat and Mass Transfer (Ref. 2), Table 8-2, p. 117.

†See the appendix for the evaluation scheme; there are slight differences from the original values of Ref. 12.

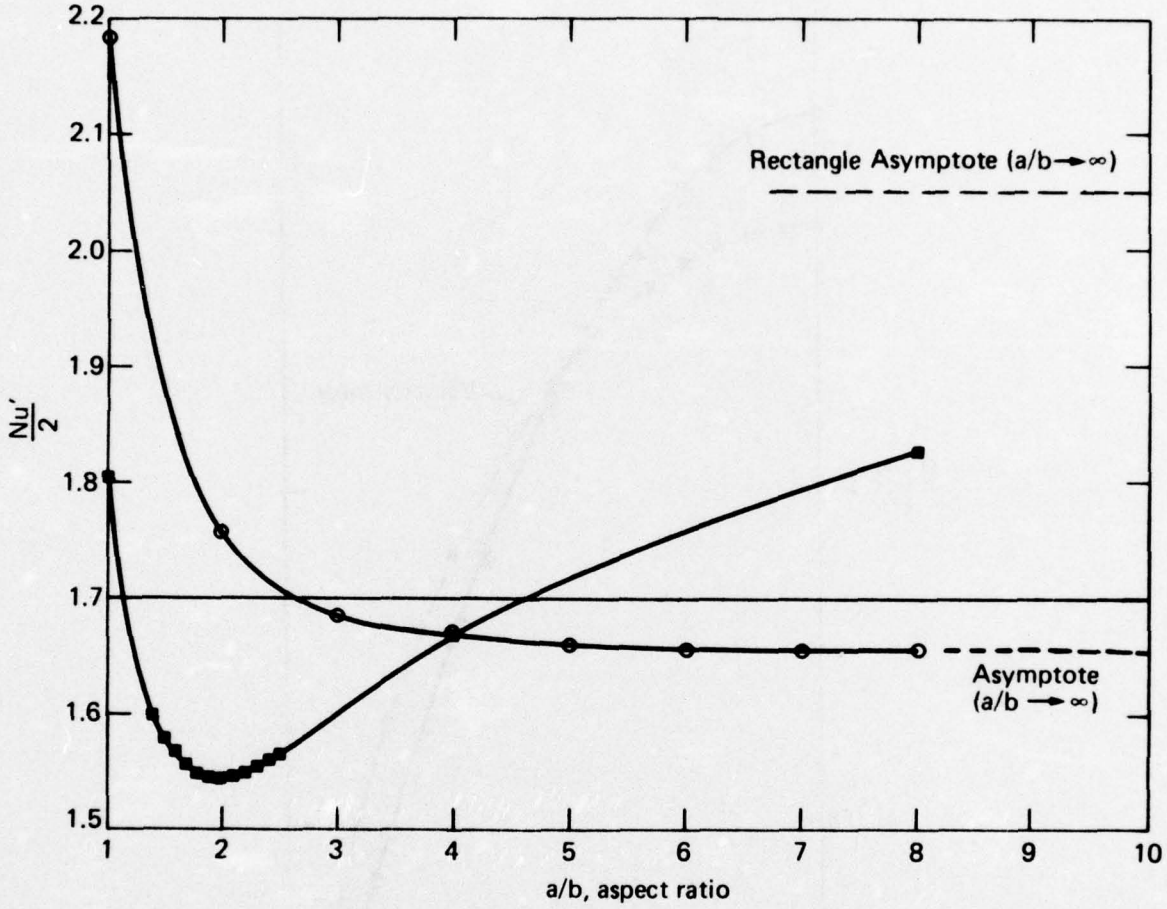

Fig. 11 **Average Thermal Barrier Inverse (Nu'/2) as a Function of Aspect Ratio a/b for Open Rectangular Ducts and Open Ellipsoidal Ducts with Uniform Peripheral Temperature**

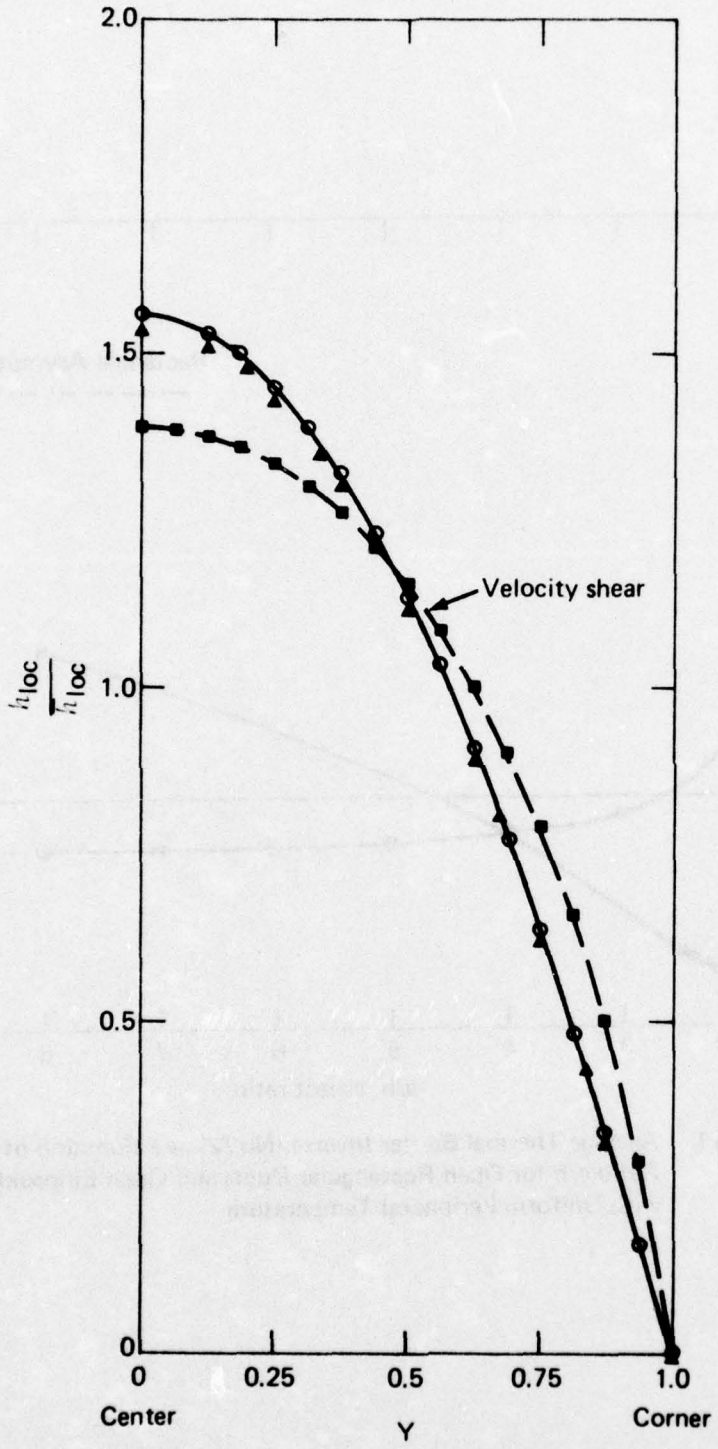

Fig. 12 Local Heat Conductance along the Perimeter of a Square Duct with Uniform Peripheral Temperature

For elliptical ducts, the shear and normal temperature gradient distributions are monotonic on the quarter-perimeter. The maxima occur at the narrow centerplane intersections, the minima at the wide centerplane intersections, the difference between extrema increasing with eccentricity of the ellipse.

3. Heat Transfer in Ducts with Extended Surfaces

The finned ducts have increased perimeters and decreased areas compared to the open square ducts. This means the hydraulic diameter D_e is always smaller for the finned ducts. One gets the impression from the literature that this decrease in D_e is more than compensated for by more effective heat transfer.

The ordinary Nusselt number for any noncircular duct is, in the present notation,

$$Nu = \left(\frac{2A}{Pb}\right)^2 \frac{\overline{u}^*}{\theta_b^*} .$$

The corresponding form of Nu' is

$$Nu' = \left(\frac{2A}{Pb}\right) \frac{\overline{u}^*}{\theta_b^*} .$$

Values of P, A, Nu, and Nu'/2 are given in Table 4 for the finned square ducts with uniform peripheral temperature. For the thick 50% fins, the ordinary Nu is considerably smaller, while the "thermal barrier" is essentially unchanged from the open square duct. For the narrow fins of increasing length, a small disturbance of the flat wall substantially decreases Nu, but as the fin gets longer Nu recovers and exceeds the value for the open square duct. On the other hand, Nu' shows less of a decrement for small fins and considerable improvement (Nu' increasing, barrier layer decreasing) as the fin gets longer. So by both criteria only the long thin fin does achieve a more effective average heat transfer.

The level of the temperature gradient along the unmodified flat walls is always decreased by the presence of the fins, but the fins themselves contribute heavily to the flux along the finned wall. The distribution of h_{loc} is similar to the velocity gradient distribution (Fig. 13). There are discontinuities at the sharp corner of the fin due to lack of mathematical normal at the point,

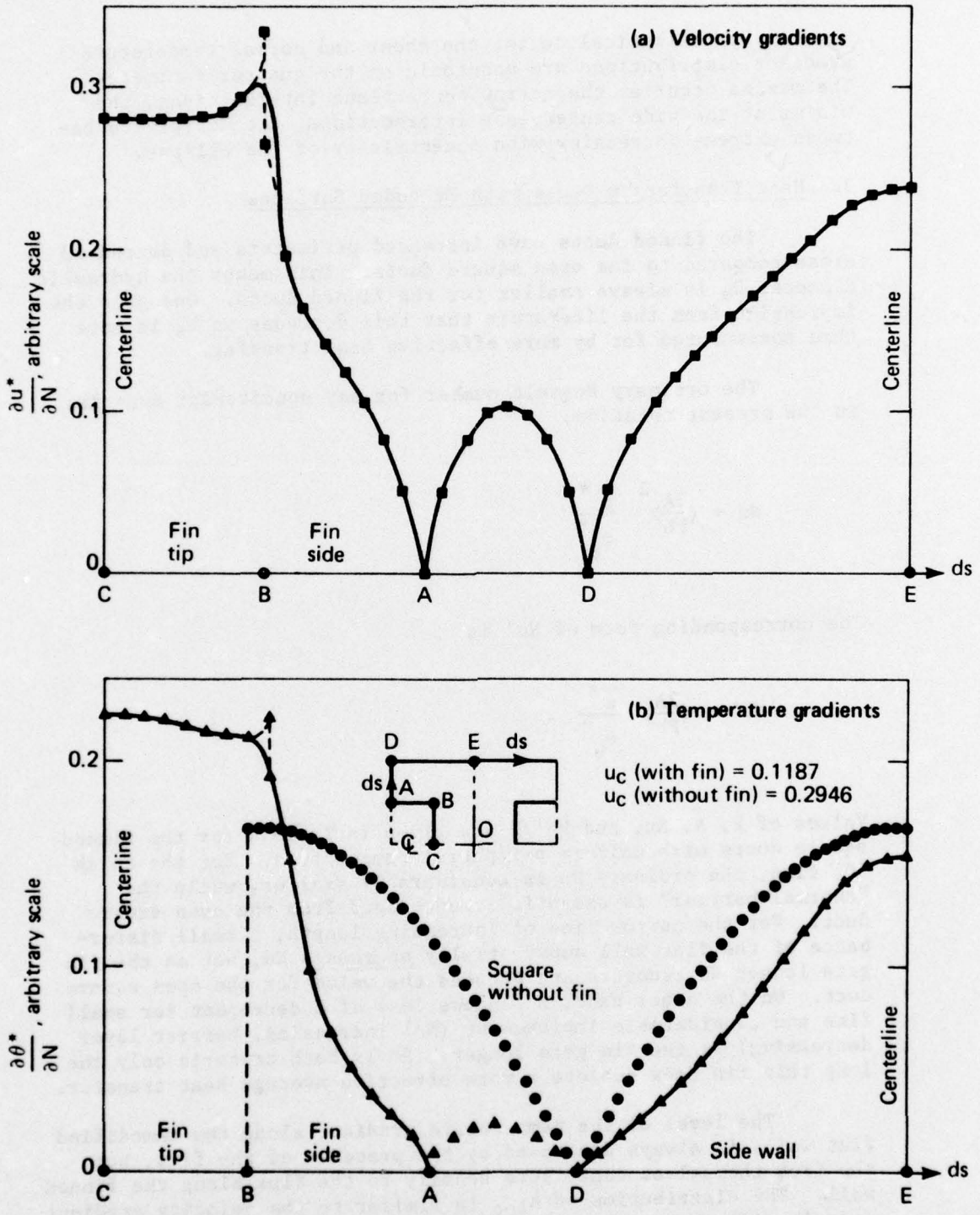

Fig. 13 Variation of Velocity Gradients (shear) and Temperature Gradients (conductance) along the Perimeter for a Finned Square Duct with Uniform Peripheral Temperature

Table 4

Average Heat-Transfer Nusselt Number for
Finned Square Ducts

d/b	Pb^{-1}	Ab^{-2}	$\bar{u}^*$	θ_b^*	Nu	Nu'/(2)
Wide Fin						
0.50	10	3	0.0353	0.00594	2.14	1.78
Narrow Fins						
0.25	9	3.75	0.0927	0.0228	2.82	1.70
0.50	10	3.5	0.0538	0.00861	3.06	2.18
0.75	11	3.25	0.0314	0.00285	3.84	3.25
No Fin						
0	8	4	0.1404	0.0390	3.60	1.80

but of course the real surfaces are smooth so a smoothed curve has been drawn locally. In the surface conductance expression, the fin effect is enhanced by the lowered value of θ_b^* as the fin length increases (see Table 4). However, the temperature gradients along the very long fin decrease in relative magnitude. The advantage of high flux from the fin (proportional to the gradient) has reached a point of diminishing return.

Similar calculations can be done with fins in rectangular or elliptical ducts with anticipated modifications from open duct heat transfer values.

4. Summary

The quantity $2A/bP \equiv (D_e/2b)$ is a measure of relative surface area that appears in the definitions of Nu and Nu'. It is instructive to plot Nu and Nu'/2 (inversely proportional to the thermal barrier length) against the relative surface area parameter to view the correlation of average heat transfer within the various ducts; this has been done in Fig. 14. The open ellipsoidal curve essentially intersects the open rectangular one, physically reasonable because D_e approaches a limit for large eccentricity (not as in Ref. 3, where $a/b \to \infty$ leads to a "physically unrealistic limit"). For open ducts of small aspect ratio a/b, the ellipse curve seems to be an upper bound, and the rectangle curve a lower

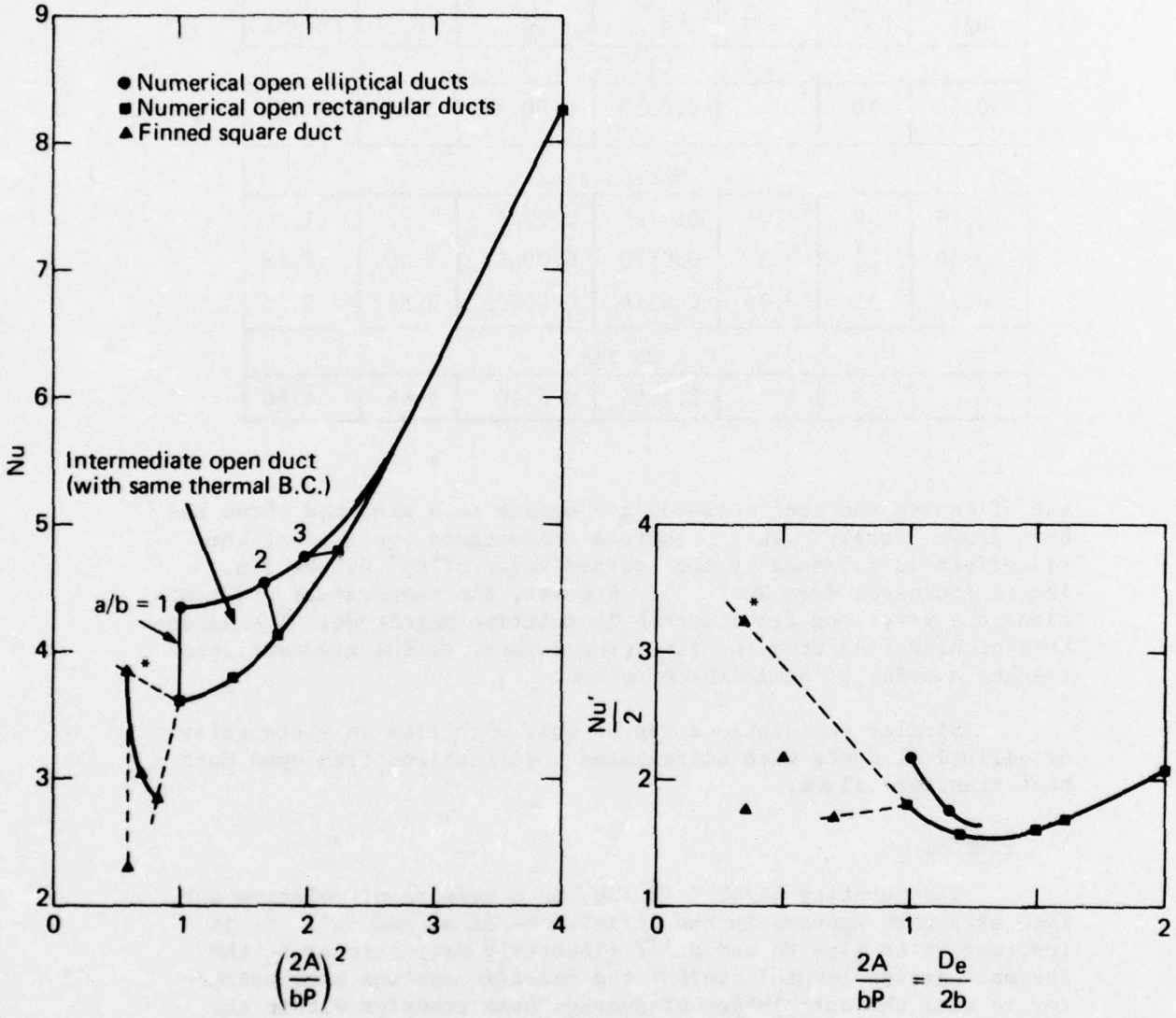

Fig. 14 Correlation of Average Heat-Transfer Parameters for Uniform Peripheral Temperature in terms of a Relative Surface Parameter, $2A/bP \equiv D_e/2b$

bound on the ordinary Nusselt number that can be obtained for any intermediate shape (rather similar to conclusions about centerline velocity for the velocity field under constant pressure gradient, Ref. 4). Intermediate duct shapes for large a/b where D_e is larger than the elliptic limit probably lie essentially on the rectangular curve. The apparently advantageous high Nu with large a/b is mostly due to the D_e factor in its definition. The average heat transfer based on true geometric diameter, Nu', is reasonably constant for all the open ducts.

The variation of Nu with a/b has been calculated elsewhere for open rectangular ducts for other homogeneous thermal boundary conditions (Refs. 1 and 2). The results have also been plotted in the coordinates of Fig. 14 producing lower Nu curves, the one with absolutely uniform wall temperature having a similar trend to D_e.

The extended surface ducts, all derivative from the square duct, are represented by triangles in Fig. 14. Most of them, although they have $(2A/bP) < 1$, have worse Nu than the open square duct, the data points following the downward trend of Nu with lower (2A/bP). The average thermal barrier length is also in the range of the open ducts. Only one point (starred) is on the leftward extrapolation of the upward trending rectangular (Nu'/2) curve. Only this finned duct is an improvement on the open duct. This indicates that merely decreasing D_e within an overall defined area ($2a \times 2b$) is not enough to ensure increased heat transfer. An engineer must be clever enough to design the fin that really is helpful and not just produce a Nusselt number that follows the average trend with D_e.

C. PERIPHERAL TEMPERATURE DISTRIBUTIONS

The numerical results show that the heat-transfer parameters are quite different in a given duct with uniform peripheral temperature and in the same duct with a distribution of temperature along the perimeter, even though the average wall temperature is the same.

The surface conductivity is proportional to the wall temperature gradient. The considerable difference in wall gradient when there are wall temperature distributions has been shown by the numerical calculations. No longer does the flux necessarily go to zero when the velocity shear goes to zero. The flux magnitude and surface conductivity are inversely proportional to θ_b^* which varies with the wall distribution. The variations of average heat-transfer parameters Nu and Nu'/2 are related only to the changes in θ_b^*, because the other factors are constant. Because

the distributions on the alternate square duct walls were similar, proportional to ε, the variation of θ_b^* with ε is linear:

$$\theta_b^* = (\theta_b^*)_0 + \theta_b^*(\varepsilon)$$

$$= \frac{1}{\overline{Au}^*} \int_A u^* [\theta_0^* + \theta^*(\varepsilon)] dA$$

$$= \frac{1}{\overline{Au}^*} \int_A u^* (\theta_0^* + \varepsilon\, \theta_1^*) dA \, .$$

θ_0^*, θ_1^* are found in the appendix. Results at two values of ε are sufficient to evaluate θ_b^* for all ε.

The case is similar for the temperature variation on the fins in a square duct. Here several values of β, the value of the normalized temperature at the tip corner, were assigned, and the variation of θ_b^* with β is shown to be linear in Fig. 15. There is a particular value of β ($\approx$ 0.08) when θ_b^* is zero. Since this occurs in the denominator for Nu and Nu'/2, it appears the average heat transfer is infinite for this particular fin temperature distribution (and the thermal barrier length zero). A similar particular value of ε produces the same situation in the open square duct. Further changes in β or ε produce θ_b^*'s of opposite sign. Physically this does not make sense if $\partial t/\partial x$ is a fixed (measurable) quantity; there is either average heat input to the fluid per unit length of duct or heat outflow. (A similar trouble was noted with convective problems when the fluid contained heat sources (Ref. 3); the situation was not resolved.)

The difficulty seems to be in the (arbitrary) selection of a reference temperature (see p. 4). Another convenient reference temperature might be the centerline temperature. Its variation with β is also indicated on Fig. 15. The magnitude is very nearly the same as θ_b^*. It, too, goes through zero, but at a different value of β. The only reference temperature that makes complete physical sense is the simple mean, $\overline{\theta^*}$. When that goes through zero, the average heat flow per unit length of duct does change sign. At that point the perimeter average of the local heat flux, as varied as it may be along the walls, is zero.

However, the practical interest is not near zero heat input, but large values of it. It does not appear to be a gross

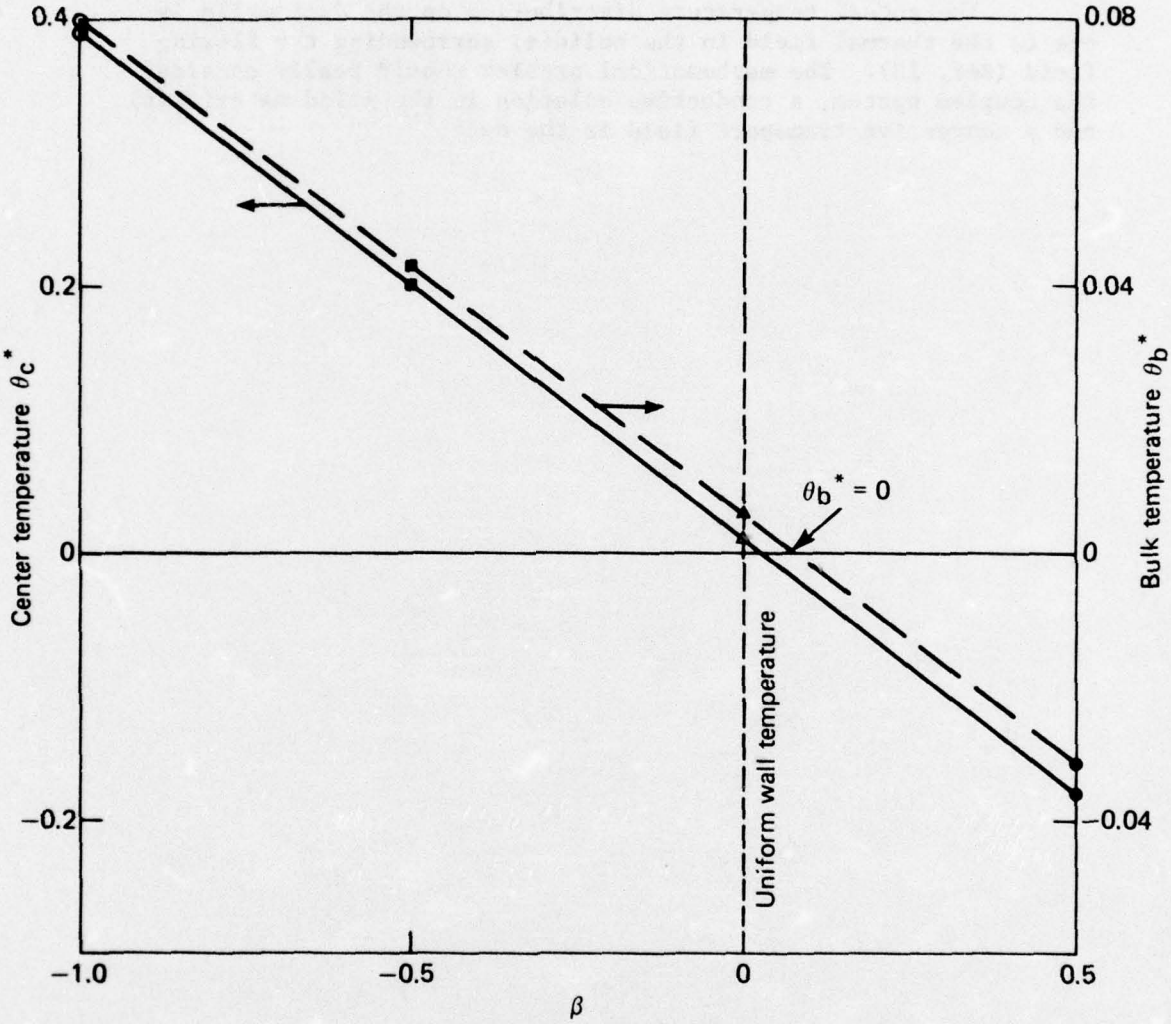

Fig. 15 "Reference" Temperatures versus Fin Corner Temperature Variation in a Square Duct with Nonuniform Temperature on Thick Fins (see Fig. 6)

error to use conventional θ_b^* to compare duct configurations with various temperature distributions unless it approaches zero. It certainly seems possible to increase the average heat transfer by introducing wall temperature distributions.

The actual temperature distribution on the duct walls is due to the thermal field in the solid(s) surrounding the flowing fluid (Ref. 13). The mathematical problem should really consider the coupled system, a conductive solution in the solid material(s), and a convective transport field in the duct.

Ref. 13. E. M. Sparrow and L. Lee, "Effects of Fin Base-Temperature Depression in a Multifin Array," Trans. ASME, Vol. 97C, 1975, pp. 463-465.

V. CONCLUSION

Enough examples of the numerical method have been shown to demonstrate its utility and to judge its worth for these particular heat-transfer problems. The Cartesian direct finite-difference convective solutions compare very favorably with accurate fully developed solutions obtained by other means. The method is adaptable for arbitrary duct cross-section shapes and allows study of various temperature conditions. Normalized conductance quantities that have been considered for heat transfer are shown to be dependent on duct shape and perimeter temperature distributions in rather complex ways, so it is difficult to make sharp statements about general trends. Specific information on wall temperature distribution is needed to answer specific questions relative to average or local heat conductance. Qualitative information on the temperature fields in irregular ducts can be drawn from the velocity field solution, if the wall conditions are similar ($\theta_w^* \sim u_w^* = 0$). Close numerical estimates can be obtained from the general Nu, Nu'/2 correlations in Fig. 14. But nonhomogeneous peripheral temperature changes the picture immensely. The examples given point to the inadequacy of the conventional bulk (mixed mean) temperature as a completely suitable reference temperature.

The method can be used in conjunction with diffusive field calculations in solids surrounding the duct, or suitable temperature measurements, to provide the complete fully developed convective thermal field in arbitrary ducts. The technique here applied to more or less rectangular shapes can easily be extended to fluted annular ducts, where consideration of extended surface length, thickness, end rounding, and number per circumference can all be handled expeditiously to optimize the convective field. Equations (1a) and (6a) can be transformed to circular cylindrical coordinates — ($\eta = \ell n\ r = \ell n\ (x^2/b^2 + y^2/b^2)^{\frac{1}{2}}$), ($\phi$) — where b is a reference radius, ϕ is azimuthal angle, and $\nabla^2 = e^{-\eta}\left(\frac{\partial^2}{\partial \eta^2} + \frac{\partial^2}{\partial \phi^2}\right)$. It should be obvious that annular numerical finite-difference programs would not be very much different from the Cartesian programs illustrated here.

ACKNOWLEDGMENT

This research was supported by the Department of the Navy, Naval Sea Systems Command, under Contract No. N00017-72-C-4401. The direct Cartesian finite-difference programs for the Laplace operator equations with the various Dirichlet boundary conditions were developed by Dr. L. W. Ehrlich, whose cheerful cooperation is gratefully acknowledged. He also made the modifications necessary to use the programs for ducts with curved boundaries. Thanks are also due to Mr. Stanley Favin, who programmed the evaluation of the exact analytic expressions for comparison purposes.

Appendix

ANALYTIC SOLUTIONS FOR FULLY DEVELOPED TEMPERATURE FIELDS IN A SQUARE DUCT WITH CONSTANT HEAT INPUT PER UNIT CHANNEL LENGTH

Although the details of analytic solution are only given here for a square duct, similar analyses can also be carried out for arbitrary rectangles. Since the primary purpose is to check the numerical solutions for accuracy, a square is sufficient to test the computer programs.

Normalizing by the central half-height of the duct, b, and with a the half-width of the duct and a ≈ b (square), the velocity solution can be written (after Ref. A-1) as

$$u^* = \frac{u}{\frac{b^2}{\mu}\frac{dp}{dz}} = \tfrac{1}{4}[2 - (X^2 + Y^2)] + \sum_{n=0}^{\infty} \frac{(-1)^{n+1}}{P_n^3}\left[\frac{\cosh P_n X}{\cosh P_n} \cos P_n Y + \frac{\cosh P_n Y}{\cosh P_n} \cos P_n X\right], \tag{A-1}$$

where $P_n = \frac{2n+1}{2}\pi$, $\frac{x}{a} = X$, and $\frac{y}{b} = Y$. (Note the symmetry in X, Y which follows the physical expectation in a square duct.) It is convenient to separate u^* into two parts, the simple polynomial plus the infinite series:

$$u^* = u_1^*(X,Y) + u_2^*(X,Y) \quad ,$$

where $\nabla^2 u_1^* = -1$ and $\nabla^2 u_2^* = 0$, which can be easily verified.

The solution to the temperature field $\theta^* = t^* - \bar{t}_w^*$ must satisfy the normalized equation

$$\nabla^2 \theta^* = u^* \quad . \tag{A-2}$$

The solution to this equation can be separated into three parts:

Ref. A-1. V. O'Brien, "Pulsatile fully-developed flow in rectangular channels," J. Franklin Inst., Vol. 300, 1975, pp. 225-230.

$$\theta^* = \theta_1^*(X,Y) + \theta_2^*(X,Y) + \theta_3^*(X,Y) \qquad \text{(A-3)}$$

where $\nabla^2\theta_1^* = u_1^*$, $\nabla^2\theta_2^* = u_2^*$, and $\nabla^2\theta_3^* = 0$.

The first part θ_1^* is a simple polynomial:

$$\theta_1^* = b_1(X^2 + Y^2) - c_1(X^2 + Y^2)^2 \qquad \text{(A-3a)}$$

$$\nabla^2\theta_1^* = 4b_1 - 16c_1(X^2 + Y^2) = \tfrac{1}{2} - \tfrac{1}{4}(X^2 + Y^2)$$

so

$$b_1 = 1/8, \; c_1 = 1/64.$$

Noting that $\nabla^2(Y \sinh \eta Y \cos \eta X) = 2\eta \cosh \eta X \cos \eta X$, we take

$$\theta_2^* = \sum_{n=0}^{\infty} \alpha_n \left(\frac{Y \sinh P_n Y}{\cosh P_n} \cos P_n X + \frac{X \sinh P_n X}{\cosh P_n} \cos P_n Y \right)$$

$$\nabla^2\theta_2^* = \sum_n 2P_n\alpha_n \left(\frac{\cosh P_n Y}{\cosh P_n} \cos P_n X + \frac{\cosh P_n X}{\cosh P_n} \cos P_n Y \right) = u_2^* , \qquad \text{(A-3b)}$$

so that

$$\alpha_n = \frac{(-1)^{n+1}}{2 P_n^4} .$$

For θ_3^* we take a series similar to u_2^*:

$$\theta_3^* = \sum_{n=0}^{\infty} \beta_n \left(\frac{\cosh P_n Y}{\cosh P_n} \cos P_n X + \frac{\cosh P_n X}{\cosh P_n} \cos P_n Y \right) \qquad \text{(A-3c)}$$

The coefficients β_n will be chosen to satisfy the assigned boundary conditions.

1. UNIFORM PERIPHERAL TEMPERATURE t_w^*

The boundary condition is $t^* - t_w^* = \theta^* = 0$ at the edges of the square duct $|Y| = 1$ and $|X| = 1$.

(i) At $Y = \pm 1$:

$$\theta^*(X,\pm 1) = \theta_1^*(X,\pm 1) + \theta_2^*(X,\pm 1) + \theta_3^*(X,\pm 1) = 0 \qquad (\text{All } -1 < X < +1)$$

$$0 = \frac{3}{8}\sum_{n=0}^{\infty}\frac{(-1)^n}{P_n}\cos P_n X - \frac{3}{4}\sum_{n=0}^{\infty}\frac{(-1)^n}{P_n^5}\cos P_n X + \sum_{n=0}^{\infty}\frac{(-1)^{n+1}}{2P_n^4}\tanh P_n \cos P_n X$$

$$+ \sum_{n=0}^{\infty}\beta_n \cos P_n X \ , \qquad \text{(A-4)}$$

where use was made of the following identities†:

$$1 = 2\sum_{n=0}^{\infty}\frac{(-1)^n}{P_n}\cos P_n X \ , \qquad \text{(A-5)}$$

$$1 - X^2 = 4\sum_{n=0}^{\infty}\frac{(-1)^n}{P_n^3}\cos P_n X \ , \qquad \text{(A-6)}$$

$$5 - 6X^2 + X^4 = 48\sum_{n=0}^{\infty}\frac{(-1)^n}{P_n^5}\cos P_n X \ . \qquad \text{(A-7)}$$

---

†These are taken from Jolley (Ref. A-2): Eq. (A-5) from #506, p. 96; Eq. (A-6) from #528, p. 100; and Eq. (A-7) derived from #345, p. 64.

Ref. A-2. L. B. W. Jolley, Summation of Series, Dover, New York, 1961.

From Eq. (A-4) we see that

$$\beta_n = \frac{3}{8}\frac{(-1)^{n+1}}{P_n} + \frac{3}{4}\frac{(-1)^n}{P_n^5} + \frac{1}{2}\frac{(-1)^n}{P_n^4}\tanh P_n \quad . \qquad \text{(A-8)}$$

(ii) At $X = \pm 1$, the same coefficients also make $\theta^* = 0$ because of the symmetry in X and Y.

For easy comparison to the numerical results, we note the center value

$$\theta^*(0,0) = \theta_3^*(0,0) = \sum_{n=0}^{\infty} \frac{2\beta_n}{\cosh P_n} = -0.06500 \quad . \qquad \text{(A-9)}$$

Another compact form of analytic solution for a square duct with the same boundary condition is known. Marco and Han (Ref. 12) give a formula involving double infinite summations.

$$\theta^*(X',Y') = \frac{16}{\pi^6}\sum_{n=0}^{\infty}\sum_{m=0}^{\infty} \frac{\sin\left(\frac{2n+1}{2}\pi X'\right)\sin\left(\frac{2m+1}{2}\pi Y'\right)}{(2n+1)(2m+1)\left[\left(\frac{2m+1}{2}\right)^2 + \left(\frac{2n+1}{2}\right)^2\right]^2} \qquad \text{(A-10)}$$

where (X',Y') are measured from the corner of the square ($0 \le X' \le 2$, $0 \le Y' \le 2$) by analogy to an existing solution for deflections of a simply supported thin plate under uniform lateral load. The velocity field u^* is also represented by a doubly infinite summation.

The Nusselt number as a function of a/b (Ref. 12) is expressed concisely in terms of double summations (A-11) and has been evaluated by a short program in APL language. (The author is indebted to Mr. Stanley Favin for the program and comments.)

$$Nu = \frac{64}{(1+\frac{a}{b})^2 \pi^2} \frac{\left(\sum_{M=1,3,5,..}^{\infty} \sum_{N=1,3,5,..}^{\infty} \frac{1}{M^2N^2\left|M^2 + N^2\left(\frac{a}{b}\right)^2\right|} \right)^2}{\sum_{M} \sum_{N} \frac{1}{M^2N^2\left|M^2 + N^2\left(\frac{a}{b}\right)^2\right|^3}} \qquad \text{(A-11)}$$

$$\left[1/2\ Nu' = \frac{1+\frac{a}{b}}{4\left(\frac{a}{b}\right)}\ Nu \right] .$$

The evaluation of Nu (a/b) with (K + 1) terms was easily programmed on an IBM computer using the APL language. The program is listed below along with comments.

```
     ∇NUCALC                    THE NAME OF THE PROGRAM.
[1]  ⎕IO←0                      SET THE ORIGIN TO ZERO.
[2]  M←N←(1+2×⍳K)*2             GENERATE TWO EQUAL VECTORS WHOSE ELEMENTS
                                        ARE THE SQUARED SEQUENCE 1,3,5,..(1+2K)
[3]  ⎕IO←1                      RESET THE ORIGIN      TO 1.
[4]  C←64÷((1+A÷B)×○1)*2        CALCULATE THE CONSTANT FACTOR:
                                                C=64/[(1+A/B)**2x PI**2]
[5]  MN←M∘.×N                   GENERATE THE OUTER PRODUCT OF M AND N.
                                MN WILL BE A K×K MATRIX OF NUMBERS REPRESENTING
                                M**2×N**2 INSIDE THE DOUBLE SUMS.
[6]  MNA←M∘.+N×(A÷B)*2          MNA WILL BE A K×K MATRIX OF NUMBERS REPRESENTING
                                M**2 + N**2×(A/B)**2 INSIDE THE DOUBLE SUMS.
[7]  TOP←(+/,÷MN×MNA)*2         TOP IS THE DOUBLE SUM SQUARED IN  THE NUMERATOR
                                OF THE EQUATION.
[8]  BOT←+/,÷MN×MNA*3           BOT IS THE DOUBLE SUM IN THE DENOMINATOR.
[9]  NU←C×TOP÷BOT               NU
[10] 'NU = ';NU;'   NU¯/2 = ';NU×(1+A÷B)÷4×A÷B     PRINT THE ANSWERS.
     ∇                          THE END.
```

2. BOUNDARY TEMPERATURE DISTRIBUTION

The differential equation is still Eq. (A-2) but the solution sought must satisfy $\theta^* = \theta_B^*$ at the boundary, where $\bar{\theta}_B^* = 0$. Let the solution which satisfies $\theta^* = 0$ on the boundary (section (1) above) be denoted θ_0^*. Then we seek $\theta^* - \theta_0^* \equiv \eta(\varepsilon)$ where

$$\nabla^2 \eta(\varepsilon) = 0 \qquad \text{(A-12)}$$

with B.C. $\eta_B = \theta_B^*$. The symbol ε is used because the assumed symmetric boundary distributions will be characterized by the number ε, and the resulting solution will be directly proportional to ε.

$$\text{At walls } |Y| = 1, \text{ let } \theta_B^*(X) = \varepsilon(3X^2 - 1); \qquad \text{(A-13a)}$$

$$\text{at walls } |X| = 1, \text{ let } \theta_B^*(Y) = \varepsilon(3Y^2 - 1). \qquad \text{(A-13b)}$$

The expression in (A-13a) is a simple quadratic in X which can be expressed as

$$\theta_B^*(X) = (-3\varepsilon) \sum_{n=0}^{\infty} \frac{4(-1)^n}{P_n^3} \cos P_n X + 2\varepsilon \sum_{n=0}^{\infty} \frac{2(-1)^n}{P_n} \cos P_n X \ ,$$

so if

$$\theta_3^*(\varepsilon) = \sum_{n}^{\infty} \beta_n(\varepsilon) \left(\frac{\cosh P_n Y}{\cosh P_n} \cos P_n X + \frac{\cosh P_n X}{\cosh P_n} \cos P_n Y \right) = \eta(\varepsilon) \ ,$$

$$\sum_{n=0}^{\infty} \cos P_n X \left[\frac{12\varepsilon(-1)^{n+1}}{P_n^3} + \frac{4\varepsilon(-1)^n}{P_n} - \beta_n(\varepsilon) \right] = 0 \ ,$$

whence

$$\beta_n(\varepsilon) = \frac{4\varepsilon}{P_n} \left[(-1)^n + \frac{3(-1)^{n+1}}{P_n^2} \right] .$$

By symmetry in X and Y, the boundary condition of Eq. (A-13b) is also satisfied.

$$\text{The central value } \theta^*(0,0) = \theta_0^*(0,0) + \sum_{n=0}^{\infty} \frac{2\beta_n(\varepsilon)}{\cosh P_n} \, .$$

The equations are linear; the additional solutions η are directly proportional to the value of ε. All derivative η quantities are likewise proportional to ε; these include not only $\theta^*(0,0)$ but <u>bulk</u> temperature θ_b^*, temperature gradients $(\partial\theta^*/\partial N)$ on the wall, etc. Thus if $\varepsilon < 0$, the central temperature can change sign (even though the average heat flux is still positive), and even θ_b^* can become zero.

Less symmetric assigned boundary conditions on the square boundary including polynomials of any degree can be handled in similar fashion.

LIST OF SYMBOLS

A	Cross-sectional area of duct (m^2)
a	Horizontal semidiameter of duct section (m)
b	Vertical semidiameter of duct section (m); characteristic length (Fig. 1)
c_p	Specific heat of fluid (W·s/g,°C)
d	Depth of fin (m)
D_e	Hydraulic diameter (m)
h	Finite-difference mesh
h	Thermal conductance (W/m^2, °C)
k	Thermal conductivity of fluid (W/m, °C)
N	Normal direction to wall surface
Nu	Conventionally defined Nusselt number (p. 33)
Nu'	Unconventionally defined Nusselt number (p. 34)
P	Duct section perimeter (m)
p	Pressure (dyn/m^2)
Q	Volume heat addition per unit channel length (W/m^2)
S'	Diagonal stretched coordinate (p. 22)
t	Temperature (°C)
t^*	Normalized temperature (Eq. (6b))
u	z-ward velocity component (m/s)
u^*	Normalized velocity component (Eq. (1b))
x,y,x	Cartesian coordinates (m)

X,Y	Normalized Cartesian coordinates (xb^{-1}, yb^{-1}, respectively)
α	Thermal diffusivity of fluid (m/s)
β	Tip fin corner temperature (normalized)
ε	Parameter characterizing peripheral wall temperature (Eq. (A-13))
η	Convective temperature field due to peripheral wall temperature distribution (appendix)
θ^*	Normalized temperature difference ($t^* - t_w^*$)
μ	Viscosity coefficient (g/m s)
ρ	Fluid density (g/m^3)

Superscripts

$\overline{(\,)}$	Sectional average
*	Normalized quantity
'	Modified coordinate (or parameter)

Subscripts

b	Bulk (or mixed mean) value
B	Boundary value (appendix)
c	Central value
w	Wall value
ref	Reference temperature
loc	Local (surface) value
m	Summation index (appendix)
n	Summation index (appendix)

REFERENCES

1. E. M. Sparrow and R. Siegel, "A Variational Method for Fully Developed Laminar Heat Transfer in Ducts," Trans. ASME, Vol. 79C, 1959, pp. 157-167.

2. W. M. Kays, Convective Heat and Mass Transfer, McGraw Hill, New York, 1966.

3. L. N. Tao, "On Some Laminar Forced-Convection Problems," Trans. ASME, Vol. 83C, 1961, pp. 446-472.

4. V. O'Brien, "Steady and Unsteady Flow in Non-Circular Straight Ducts" (accepted by ASME J. Appl. Mech., 1976).

5. K. A. Gardner, "Efficiency of Extended Surface," Trans. ASME, Vol. 67, 1945, pp. 621-627.

6. S. H. Clark and W. M. Kays, "Laminar-Flow Forced Convection in Rectangular Tubes," Trans. ASME, Vol. 75, 1953, pp. 859-866.

7. J. M. Savino and R. Siegel, "Laminar Forced Convection in Rectangular Channels with Unequal Heat Addition on Adjacent Sides," Int. J. Heat Mass Transf., Vol. 7, 1964, pp. 733-741.

8. P. Moon and D. C. Spencer, Field Theory for Engineers, D. Van Nostrand, Princeton, 1961.

9. L. W. Ehrlich, "Solving the Biharmonic Equation as Coupled Finite Difference Equations," SIAM J. Num. Anal., Vol. 8, 1971, pp. 278-287.

10. M. H. Hu and Y. P. Chang, "Optimization of Finned Tubes for Heat Transfer in Laminar Flow," Trans. ASME, Vol. 95C, 1973, pp. 332-338.

11. R. N. Norris and D. D. Streid, "Laminar-flow Heat Transfer Coefficients for Ducts," Trans. ASME, Vol. 62, 1940, pp. 525-541.

12. S. M. Marco and L. S. Han, "A Note on Limiting Laminar Nusselt Number in Ducts with Constant Temperature Gradient by Analogy to Thin-Plate Theory," Trans. ASME, Vol. 77, 1955, pp. 625-630.

13. E. M. Sparrow and L. Lee, "Effects of Fin Base-Temperature Depression in a Multifin Array," Trans. ASME, Vol. 97C, 1975, pp. 463-465.

A-1. V. O'Brien, "Pulsatile fully-developed flow in rectangular channels," J. Franklin Inst., Vol. 300, 1975, pp. 225-230.

A-2. L. B. W. Jolley, Summation of Series, Dover, New York, 1961.

INITIAL DISTRIBUTION EXTERNAL TO THE APPLIED PHYSICS LABORATORY*

The work reported in TG 1303 was done under Navy Contract N00017-72-C-4401.
This work is related to Task X81K, which is supported by NAVSEASYSCOM.

ORGANIZATION	LOCATION	ATTENTION	No. of Copies
DEPARTMENT OF DEFENSE			
DDC	Alexandria, VA		12
Department of the Navy			
NAVSEASYSCOM	Washington, DC	SEA-033	1
		SEA-0341	1
		SEA-035	1
		SEA-09G3	2
NAVAIRSYSCOM	Washington, DC	AIR-50174	2
NAVPRO	Laurel, MD 20810		1
Naval Ship R&D Center	Washington, DC	H. J. Lugt	1
		J. W. Schot	1
		F. N. Frenkiel	1
Naval Postgraduate School	Monterey, CA	T. Sarpkaya	1
CONTRACTORS			
Hydronautics	Laurel, MD	M. P. Tulin	1
		G. Mehta	1
Science Applications, Inc.	122 La Veta, N.E. Albuquerque, NM 87108	P. J. Roache	1
UNIVERSITIES			
MIT	Cambridge, MA 02139	K. A. Smith, Dept. Chem. Engr.	1
Pennsylvania State U.	University Park, PA 16802	N. Davids, Dept. Engr. Sci. & Mech.	1
Ohio State U.	Columbus, OH 43210	R. M. Nerem, Biomed. Engr. Ctr.	1
Washington U.	St. Louis, MO 63130	S. P. Sutera, Dept. Mech. & Aero. Engr.	1
Case Western Reserve U.	Cleveland, OH 44106	I. Greber, Dept. Fluid, Theor., Aero. Sci.	1
		E. Reshotko, School of Engr.	1
City U. of New York	NY, NY 10021	S. Weinbaum, Dept. Mech. Engr.	1
U. of Notre Dame	Notre Dame, IN 46556	T. J. Mueller, Dept. Aero. & Mech. Engr.	1
U. of Minnesota	Minneapolis, MN 55455	D. D. Joseph, Dept. Mech. & Aero. Engr.	1
		E. M. Sparrow, Dept. Mech. & Aero. Engr.	1
U. of Pennsylvania	Philadelphia, PA 19104	E. B. Dussan, Chem. Engr.	1
Cornell U.	Grumman Hall Ithaca, NY 14850	K. E. Torrance, Sibley Sch. Mech. & Aero. Engr.	1
Stanford U.	Stanford, CA 94305	H. Brenner, Chem. Engr.	1
		A. Acrivos, Chem. Engr.	1
		U. B. Mehta, Chem. Engr.	1
Illinois Inst. of Technology	Chicago, IL	Z. Lavan	1
		M. V. Morkovin	1
Columbia U.	NY, NY 10027	R. Skalak, Dept. Civil Engr. & Engr. Mech.	1
Catholic U.	Washington, DC 20017	H. B. Atabek	1
Johns Hopkins U.	Baltimore, MD 21218	S. Davis, Dept. Mech. & Material Sci.	1
		S. Corrsin, Dept. Mech. & Material Sci.	1
Clarkson College of Technology	Potsdam, NY 13676	F. F. Erian, Dept. Mech. Engr.	1
Technion	Haifa, Israel	S. Irmay, Dept. Hydrau. Engr.	1
		G. Hetsroni, Dept. Mech. Engr.	1

Requests for copies of this report from DoD activities and contractors should be directed to DDC, Cameron Station, Alexandria, Virginia 22314 using DDC Form 1 and, if necessary, DDC Form 55.

***Initial distribution of this document within the Applied Physics Laboratory has been made in accordance with a list on file in the APL Technical Publications Group.**